Influence of small-scale turbulence on internal flamelet structure

Citation for the original published paper (version of record):
Lipatnikov, A., Sabelnikov, V. (2023). Influence of small-scale turbulence on internal flamelet structure. Physics of Fluids, 35(5). http://dx.doi.org/10.1063/5.0153089

(article starts on next page)

A priori test of perfectly stirred reactor approach to evaluating mean fuel consumption and heat release rates in highly turbulent premixed f lames

Citation for the original published paper (version of record):
Lipatnikov, A., Sabelnikov, V. (2023). A priori test of perfectly stirred reactor approach to evaluating mean fuel consumption and
heat release rates in highly turbulent premixed f lames. Physics of Fluids, 35.
http://dx.doi.org/10.1063/5.0153089

Accepted to Phys. Fluids 10.1063/5.0153089

Influence of small-scale turbulence on internal flamelet structure

Andrei N. Lipatnikov[a,1], Vladimir A. Sabelnikov[b,c]
[a]Department of Mechanics and Maritime Sciences, Chalmers University of Technology, Gothenburg, 41296 Sweden
[b]ONERA – The French Aerospace Laboratory, F-91761 Palaiseau, France
[c]Central Aerohydrodynamic Institute (TsAGI), 140180 Zhukovsky, Moscow Region, Russian Federation

Abstract
Direct numerical simulation data obtained from a highly turbulent (Kolmogorov length scale is less than a laminar flame thickness by a factor of about 20) lean hydrogen-air complex chemistry flame are processed, with the focus of the study being placed on flame and flow characteristics conditioned to instantaneous local values $c_F(\mathbf{x},t)$ of the fuel-based combustion progress variable. By analyzing such conditioned quantities, the following two trends are documented. On the one hand, magnitudes of fluctuations of various local flame characteristics decrease with increasing the combustion progress variable, thus, implying that the influence of small-scale (when compared to the laminar flame thickness) turbulence on internal flamelet structure is reduced as the flow advance from unburned reactants to combustion products. On the other hand, neither local turbulence characteristics (conditioned rms velocities, total strain, and enstrophy) nor local characteristics of flame-turbulence interaction (flame strain rate) decrease substantially from the reactant side to the product side. To reconcile these two apparently inconsistent trends, the former is hypothesized to be caused by the following purely kinematic mechanism: residence time of turbulence within a large part of a local flamelet is significantly shortened due to combustion-induced acceleration of the local flow in the direction normal to the flamelet. This residence-time reduction with increasing c_F is especially strong in the preheat zone ($c_F < 0.3$) and the residence time is very short for $0.3 < c_F < 0.8$. Therefore, small-scale turbulence penetrating the latter zone is unable to significantly perturb its local structure. Finally, numerical results that indirectly support this hypothesis are discussed.

Keywords: Premixed turbulent combustion; Thermal expansion; Turbulence; Flame broadening; DNS; Hydrogen

I. INTRODUCTION

Since the pioneering work by Damköhler[1] and Shelkin,[2] substantial progress was reached in turbulent combustion modeling, e.g., see papers published recently in this journal.[3-12] Nevertheless, the combustion community has been striving to uncover governing physical mechanisms of the influence of turbulence on a premixed flame under different conditions. This goal was often pursued by introducing combustion regime diagrams[13-15] where different physical scenarios were hypothesized for different non-dimensional turbulent flame characteristics such as rms velocity u'/S_L, an integral length scale L/δ_L, Damköhler number $Da = \tau_t/\tau_f$, or Karlovitz number $Ka = \tau_f/\tau_K$ or $(\delta_L/\eta_K)^2$. Here, S_L, δ_L, and $\tau_f = \delta_L/S_L$ designate laminar flame speed, thickness, and time scale, respectively; $\tau_t = L/u'$ and τ_K are turbulence and Kolmogorov[16,17] time scales, respectively; and η_K is Kolmogorov length scale. For large-scale and weak turbulence associated commonly with $L/\delta_L \gg 1$, $u'/S_L = O(1)$, $Da \gg 1$, and $Ka < 1$, there is consensus that the influence of turbulence on a premixed flame consists primarily in wrinkling flame surface, thus, increasing its area and bulk burning rate.[18-20] For intense turbulence characterized by a small Da, a large $(\delta_L/\eta_K)^2$, and $u'/S_L \gg 1$, there is no consensus and

[1]Corresponding author, lipatn@chalmers.se

different scenarios are still discussed. Under such conditions, large-scale turbulent structures, i.e., structures whose length scale is substantially larger than the thickness δ_L, are still considered to increase flame surface area by stretching the surface. Moreover, stretch rates created by such large-scale turbulence can change local flame structure and even extinguish combustion locally. However, the large-scale turbulence can neither penetrate local flames nor directly increase magnitudes of fluctuations of various mixture characteristics (e.g., density, temperature, species mass fractions, or reaction rates) within local flames (i.e., fluctuation magnitudes conditioned to the local values of a combustion progress variable). On the contrary, small-scale turbulent structures, i.e., structures whose length scale is smaller than δ_L, could penetrate local flames, thus, intensifying mixing and increasing fluctuation magnitudes inside them. While such small-scale effects are widely expected to exist under certain conditions, there is consensus neither regarding particular manifestations of these effects nor regarding conditions under that such manifestations are of importance.

More specifically, in the first combustion regime diagrams, broadening of local flames by small-scale turbulence was hypothesized under conditions of $\eta_K < \delta_L$.[13,15] If (i) $\eta_K = LRe_t^{-3/4}$, (ii) $\tau_K = \tau_t Re_t^{-1/2}$, and (iii) $\delta_L = \nu_u/S_L$, as often assumed,[13-15] a criterion of $\eta_K < \delta_L$ reads $Ka > 1$. Here, $Re_t = u'L/\nu_u$ is turbulent Reynolds number and ν_u is kinematic viscosity of unburned mixture. Later, Peters[21] emphasized that reaction zones could remain thin if $\delta_r < \eta_K < \delta_L$, because the reaction zone thickness $\delta_r \ll \delta_L$ within the framework of the classical thermal theory[22] of laminar premixed flames. By assuming that $\delta_r/\delta_L = 0.1$, Peters[18,21] suggested a criterion of $Ka = 100$ to be an upper boundary of thin reaction zone regime provided that simplifications (i)-(iii) held. However, since complex-chemistry flames are characterized by significantly larger δ_r/δ_L, with this ratio being as large as 0.5 in moderately lean and near stoichiometric hydrogen-air flames, that boundary should be associated with significantly lower Karlovitz numbers.[23] Nevertheless, the criterion $Ka = 100$ was widely accepted over almost two decades, with both local broadening of preheat zones and existence of thin reaction zones being documented in experimental and Direct Numerical Simulation (DNS) studies, reviewed elsewhere.[24-26] Accordingly, appearance of thickened reaction zones at $Ka > 100$ was often assumed, but evidence of such a regime is still rare.

On the contrary, recent measurements and DNSs put the utility of criteria of both $Ka = 1$ (broadening of preheat zones) and $Ka = 100$ (broadening of reaction zones) into question. First, various experimental and DNS data reviewed elsewhere[25,26] indicate that reaction zones are thin even if η_K is much smaller than δ_r. In the latest measurements,[27,28] thin reaction zones were documented at Ka significantly larger than 100, while broadened reaction zones were also reported at $Ka = 590$ by Fan et al[28] (while a value of Ka is sensitive to its definition,[23] definitions adopted by Peters[18,21] and by Fan et al.[27,28] are consistent).

Second, a recent experimental study by Skiba et al.[29] has shown that a criterion of broadening of flame preheat zones by small-scale turbulence should quantitatively and qualitatively differ from $Ka = 1$, with the influence of turbulent structures smaller than δ_L on the internal structure of such zones being weak under conditions of those measurements.

Moreover, there are other data that imply weak influence of small-scale (when compared to δ_L) turbulence on premixed flames. For instance, by running 2D numerical simulations of interactions of a laminar premixed flame and a vortex pair, Poinsot et al.[30] have shown that too small vortices decay rapidly and do not substantially perturb the flame. Subsequent numerical and experimental research into this and similar problems (e.g., interactions of a laminar premixed flame and a single vortex) supported the above conclusion, as reviewed elsewhere,[31] and reported also in recent papers.[32,33]

Besides, Poludnenko and Oran[34] simulated highly turbulent premixed flames by adopting numerical meshes with different cell sizes to vary the small-scale branch of turbulence spectrum (in the cited study, kinematic viscosity was set equal to zero and turbulence spectra were bounded by numerical diffusion, which depended directly on the cell size). Reported results did not show substantial perturbations of internal structure of reaction zones even when energy cascade simulated in nonreactive turbulence extended to length scales significantly smaller than δ_r. While moderate broadening of flame preheat zones was documented in certain cases, the authors have concluded[34] that "*the action of small-scale turbulence is suppressed throughout most of the flame*" and "*small-scale motions in cold fuel do not affect the evolution of the flame brush*".

Furthermore, numerical results obtained by Aspden[35] by artificially varying mixture viscosity in a DNS series do not show substantial influence of the viscosity on 2D slices of fuel concentration, temperature, and fuel consumption rate, while vorticity fields simulated in different cases are significantly different. Accordingly, Aspden[35] discussed "*suppression of turbulence through the flame*" and attributed this effect mainly to "*fluid expansion through the flame*".

In addition, Doan et al.[36] analyzed DNS data to compare contributions of turbulent structures of different scales to flame straining and reported that the studied flames were primarily strained by structures whose length scale was larger than $2\delta_L$.

Thus, there is a plenty of evidence of inability of turbulent structures whose length scales are smaller than thickness of flame preheat zones to substantially affect the internal structure of such zones and to broaden them. Such findings are often attributed to decay of small-scale turbulence within flame preheat zones[24,26,29] due to (i) the local increase in the temperature and, hence, the mixture viscosity and (ii) an increase in the eddy size due to thermal expansion. Both physical mechanisms cause an increase in the length scale of the smallest eddies, thus, resulting in disappearance or weakening of these eddies. The latter physical mechanism may be prioritized based on the aforementioned DNS data by Poludnenko and Oran[34] and by Aspden.[35]

While a hypothesis about decay (disappearance or weakening) of the smallest turbulent eddies within flame preheat zones appears to be convincing from qualitative perspective and, therefore, is widely accepted, the present authors are aware of a single study aiming at exploring this hypothesis in turbulent flows, where evolution of small-scale turbulence is affected not only by viscous and thermal expansion effects, but also by kinetic energy transfer from larger eddies (such a flux does not appear during interactions of a single vortex or vortex pair with a laminar premixed flame). Wabel et al.[37] performed 2D measurements of variations of several turbulence characteristics (kinetic energy, strain rate, and a "conditioned" integral length scale) in the vicinity of reaction zones of highly turbulent flames. The reported results do not show a substantial decay of the turbulent kinetic energy in flame preheat zones but do show an increase in the length scale in such zones. These findings were interpreted to indicate decay of small-scale turbulence in flame preheat zones. However, the study did not provide direct evidence of this decay, because the smallest-scale turbulent eddies could not be resolved using the state-of-the-art optical diagnostic tools under conditions of these measurements.

Thus, evolution of small-scale (when compared to δ_L) turbulence in flame preheat zones and influence of this turbulence on the inner structure of such zones and their surface area still challenge the combustion community. The present work addresses these fundamental issues by analyzing DNS data obtained earlier by Dave et al.[38,39] from a turbulent, complex-chemistry, lean hydrogen-air flame. In the next section, the DNS attributes and applied numerical diagnostic techniques are summarized. Numerical results are reported and discussed in Sec. III, followed by conclusions.

II. DNS ATTRIBUTES AND PROCESSING METHODS

Since the DNS attributes were already reported in earlier papers,[38-43] only a summary is provided below. A statistically planar, moderately lean H_2/air turbulent flame in a box (19.18 × 4.8 × 4.8 mm) was simulated invoking a detailed chemical mechanism (21 reactions between 9 species) by Li et al.[44] and the mixture-averaged model of molecular transport. The equivalence ratio, unburned gas temperature, and pressure were set equal to 0.81, 310 K, and 0.1 MPa, respectively. Under such conditions, $S_L = 1.84$ m/s, $\delta_L = (T_b - T_u)/\max|\nabla T| = 0.36$ mm, and $\tau_f = 0.20$ ms. Here, subscripts u and b designate unburned and burned gas, respectively.

Three-dimensional unsteady compressible governing equations (i.e., continuity, Navier-Stokes, energy and species transport equations) were numerically solved adopting the Pencil code[45] and a numerical mesh of $960 \times 240 \times 240$ cells. At the inlet and outlet, Navier-Stokes characteristic boundary conditions[46] were set. At four other sides, the boundary conditions were periodic.

Homogeneous isotropic turbulence was pre-generated using large-scale forcing and fully periodic boundary conditions in a cube. Subsequently, the turbulence evolved until a statistically stationary state with Kolmogorov-Obukhov's 5/3-spectrum was reached.[38] During combustion simulations initiated by embedding a planar laminar flame into the computational domain at $x = x_0$ and $t = 0$, this turbulence entered the computational domain at a constant mean velocity through the left boundary. The injected turbulence decayed along the x-axis. The flame propagated in the opposite direction against a turbulent flow.

The pre-generated turbulence was characterized[39] by $u' = 6.7$ m/s, $L = 3.1$ mm, $\eta_K = (\nu_u^3/\langle\varepsilon\rangle)^{1/4} = 0.018$ mm, $\tau_K = (\nu_u/\langle\varepsilon\rangle)^{1/2} = 0.015$ ms, and $Re_t = u'L/\nu_u = 950$. Here, $\langle\varepsilon\rangle = \langle 2\nu S_{ij}S_{ij}\rangle$ is the dissipation rate, averaged over the cube; $S_{ij} = \left(\partial u_i/\partial x_j + \partial u_j/\partial x_i\right)/2$ is the rate-of-strain tensor; the summation convention applies to repeated indexes. At the leading edge of the mean flame brush, associated here with transverse-averaged temperature-based combustion progress variable $\bar{c}_T(x) = 0.01$, the turbulence characteristics were different, i.e., $u' = 3.3$ m/s, Taylor length scale $\lambda = \sqrt{10\nu_u\bar{k}/\bar{\varepsilon}} = 0.25$ mm or $0.69\delta_L$, $\eta_K = 0.018$ mm or $0.05\delta_L$, and $\tau_K = 0.087$ ms. Accordingly, $Re_\lambda = u'\lambda/\nu_u = 55$, $Ka = 2.3$, while $(\delta_L/\eta)^2$ is about 400. The difference in Ka and $(\delta_L/\eta)^2$ is very large, because $S_L\delta_L/\nu_u \gg 1$ in moderately lean H_2-air mixtures.[23]

Average quantities and Probability Density Functions (PDFs) reported in the next section are conditioned to the local values $c_F = \left(Y_F - Y_{F,u}\right)/\left(Y_{F,b} - Y_{F,u}\right)$ of fuel-based combustion progress variable, where Y_F designates fuel mass fraction. For instance, the conditioned value $\langle q|\xi\rangle$ of the quantity q is sampled as follows

$$2\langle q|\xi\rangle(\xi,t) = \iiint q(\mathbf{x},t)I(\mathbf{x},t,\xi)d\mathbf{x}, \quad (1)$$

where the indicator function $I(\mathbf{x},t,\xi) = \mathrm{H}[c_F(\mathbf{x},t) - \xi + \Delta\xi] - \mathrm{H}[c_F(\mathbf{x},t) - \xi - \Delta\xi]$ is equal to unity if $\xi - \Delta\xi < c_F(\mathbf{x},t) < \xi + \Delta\xi$ and vanishes otherwise, H designates Heaviside function, and $0 \leq \xi \leq 1$ is sampling variable. Similarly, a conditioned PDF $P(q,\xi)$ is solely yielded by a narrow zone where $I(\mathbf{x},t,\xi) = 1$ or $\xi - \Delta\xi < c_F(\mathbf{x},t) < \xi + \Delta\xi$. Such zones are very thin, because $\Delta\xi = 0.005$, i.e., 100 bins are adopted for $c_F(\mathbf{x},t)$, as well as for all other quantities $q(\mathbf{x},t)$ whose PDFs are sampled. Thus, data conditioned, e.g., to $c_F(\mathbf{x},t) = 0.5$ are sampled from zones where $0.495 < c_F(\mathbf{x},t) < 0.505$. Turbulent fluctuations inside so thin zones are controlled by small-scale turbulent structures.

Results reported in the following were sampled at 55 instants from 1.291 ms till 1.566 ms.

III. RESULTS AND DISCUSSION

Figure 1 reports PDFs of local temperature $T(\mathbf{x},t)$, local mass fraction $Y_\mathrm{H}(\mathbf{x},t)$ of atomic hydrogen, and local heat release rate $\dot{\omega}_T(\mathbf{x},t)$, conditioned to the local values of $c_F(\mathbf{x},t)$. Each of these quantities is normalized using its value taken at the same $c_F = c_F(\mathbf{x},t)$ in the unperturbed (stationary, planar, and one-dimensional) laminar premixed flame. For instance, the local temperature plotted for $c_F = 0.5$ is normalized using 1002 K, with the adiabatic combustion temperature being equal to 2177 K in the studied case.

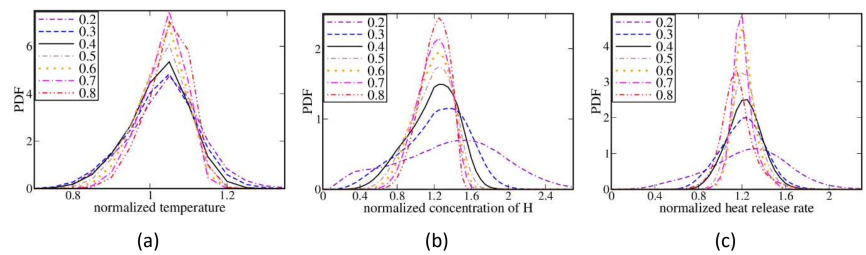

Fig. 1. Probability density functions of normalized (a) temperature, (b) mass fraction of H, and (c) heat release rate, conditioned to the local values of $c_F(\mathbf{x}, t)$ specified in legends and sampled from the entire computational domain at 55 instants. Normalization has been done using the value of the considered quantity at the same c_F in the unperturbed laminar flame.

The sampled conditioned PDFs become narrower with increasing $c_F(\mathbf{x}, t)$, at least if $c_F \le 0.7$ (this is better seen by comparing the PDF peaks at various c_F). This trend indicates a decrease in the range (magnitude) of fluctuations of the considered local flame characteristics, with such fluctuations being conditioned to narrow spatial zones and, hence, being controlled by structures whose length scale is smaller than the laminar flame thickness. Therefore, the results plotted in Fig. 1 imply reduction of the influence of the small-scale turbulence on the internal structure of local flamelets as the fluid advances from the reactants to the products. This trend is well (less) pronounced for $Y_{\mathrm{H}}(\mathbf{x}, t)$ and $\dot{\omega}_T(\mathbf{x}, t)$ (temperature, respectively), especially, when c_F increases from 0.2 to 0.4. Here, different eventual physical mechanisms, e.g., intensification of mixing or change or reaction rates, are not separated, but solely the total influence of turbulence on the PDFs is considered. Since the studied PDFs degenerate to the Dirac delta function $\delta(x-1)$ in the laminar flame, the PDF thickness directly characterizes such a total influence. Moreover, since conditioned dependencies of $\langle Y_k|\xi\rangle$, $\langle T|\xi\rangle$, $\langle \rho|\xi\rangle$, and the rates $\langle \dot{\omega}_k|\xi\rangle$ of production/consumption of various species on ξ, sampled from the studied turbulent flame, are close to the counterpart dependencies obtained from the unperturbed laminar flame,[40,41] instantaneous local flames may be associated (statistically) with flamelets under conditions of the present study, with the influence of turbulence on the conditioned rates $\langle \dot{\omega}_k|\xi\rangle$ being statistically weak. Such an association is also supported by sufficiently small widths of PDFs plotted for $c_F > 0.4$ in Fig. 1. Accordingly, instantaneous local flames are called flamelets henceforth.

In Fig. 2, a similar trend (PDF constriction with increasing c_F, which results in increasing the PDF peak with increasing c_F) is well pronounced for dilatation $\Theta \equiv \nabla \cdot \mathbf{u}$ if $0.3 < c_F < 0.7$ and for flame surface density $|\nabla c_F|$ if $0.3 < c_F < 0.8$. Here, $|\nabla c_F|$ and Θ are normalized using the laminar flame thickness δ_L and the dilatation $\Theta_L = (\sigma - 1)S_L/\delta_L$ in the laminar flame, rather than $|\nabla c_F|(c_F)$ and $\nabla \cdot \mathbf{u}(c_F)$ in the laminar flame; $\sigma = \rho_u/\rho_b$ is the density ratio.

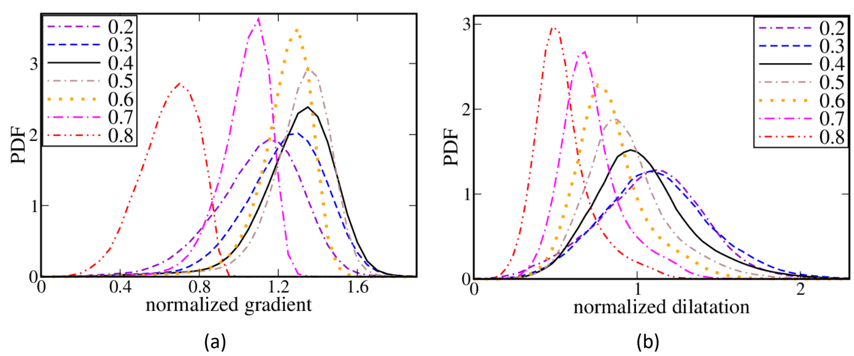

Fig. 2. Probability density functions for normalized (a) flame surface density $\delta_L|\nabla c_F(\mathbf{x},t)|$ and (b) dilatation $\Theta_L^{-1}\nabla \cdot \mathbf{u}(\mathbf{x},t)$, conditioned to the local values of $c_F(\mathbf{x},t)$ specified in legends and sampled from the entire computational domain at 55 instants.

The results reported in Figs. 1 and 2 are fully consistent with weak influence of turbulence on local structure of reaction zones, highlighted in Sect. 1. However, Figs. 3 and 4 do not allow us to attribute this weak influence to the local turbulence decay within flamelets.

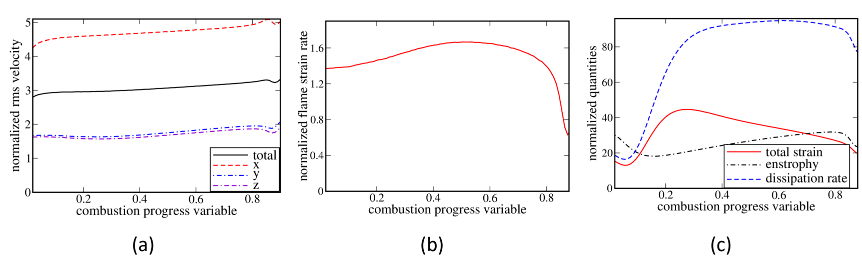

Fig. 3. (a) Normalized rms velocities. (b) Flame strain rate normalized using the laminar flame time scale τ_f. (c) Small-scale turbulence characteristics specified in legends and normalized using τ_f and ν_u. All reported quantities are conditioned to the local values of $c_F(\mathbf{x},t)$.

Indeed, first, Fig. 3a shows that the normalized conditioned rms velocities $\left(\langle u_i^2|\xi\rangle - \langle u_i|\xi\rangle^2\right)^{1/2}/S_L$, see broken lines, as well as $\langle u'|\xi\rangle/S_L \equiv \left(\sum_{i=1}^{3}\left[\langle u_i^2|\xi\rangle - \langle u_i|\xi\rangle^2\right]/3\right)^{1/2}/S_L$, see solid line, do not decrease with increasing ξ. Contrary, the observed trend is opposite at $\xi < 0.7$, while weakly pronounced. The former numerical result is consistent with experimental data by Wabel et al.[37] who did not document a decrease in the conditioned turbulent kinetic energy with a combustion progress variable either. The sole effect of combustion on the rms velocities, observed in Fig. 3a, consists of anisotropy of the fluctuating velocity field due to acceleration of the flow in the axial direction, which local flames are predominantly normal to under the studied conditions.[43]

Second, Figs. 3b and 3c indicate that the normalized flame strain rate $\tau_f\langle a_t|\xi\rangle$, see Fig. 3b, the normalized total rate of strain $\tau_f^2\langle S^2|\xi\rangle$, enstrophy $\tau_f^2\langle \omega^2|\xi\rangle$, and dissipation rate $\nu_u^{-1}\tau_f^2\langle \varepsilon|\xi\rangle$, see red solid, black dotted-dashed, and blue dashed lines, respectively, in Fig. 3c, do not show a substantial decrease with ξ if $\xi < 0.8$. Here, $a_t = \nabla\cdot\mathbf{u} - \mathbf{n}(\nabla\mathbf{u})\mathbf{n}$, $S^2 = S_{ij}S_{ij}$, $\omega^2 = \omega_i\omega_i$, and $\varepsilon = 2\nu(S^2 - \Theta^2/3)$; $\mathbf{n} = -\nabla c_F/|\nabla c_F|$ is the unit vector locally normal to flame surface and pointing to unburned reactants; and $\boldsymbol{\omega} = \nabla\times\mathbf{u}$ is vorticity vector. While the conditioned rate of strain decreases with ξ at $\xi > 0.3$, the opposite and more pronounced trend is observed at small ξ and $\tau_f^2\langle S^2|\xi = 0.8\rangle$ is still larger than $\tau_f^2\langle S^2|\xi = 0.05\rangle$.

The considered conditioned small-scale turbulence and flame characteristics decrease rapidly with increasing ξ at $\xi(\mathbf{x},t) > 0.8$. Such large values of ξ are associated with a radical recombination zone, where the temperature is gradually increases due to relatively low heat release in three-molecular recombination reactions.[47] Due to a relatively large thickness of this zone, larger-scale turbulent eddies can penetrate it and perturb its structure, e.g., PDFs plotted in Figs. 1a, 1c, or 2a are wider at $\xi = 0.8$ than at $\xi = 0.7$. However, the influence of a larger scale turbulent structures on the radical recombination zone is beyond the scope of the present work, whose focus is placed on preheat and reaction zones of instantaneous local flames.

Sufficiently weak ξ-dependencies of $\tau_f^2\langle S^2|\xi\rangle$ and $\tau_f^2\langle \omega^2|\xi\rangle$, sampled from the DNS data within flamelets, are also consistent with the experimental data by Wabel et al.,[37] who reported 2D counterparts

Accepted to Phys. Fluids 10.1063/5.0153089

of S^2 and ω^2. However, those experimental data characterized moderately small velocity gradients resolved in the measurements, whereas $\tau_f^2\langle S^2|\xi\rangle$ and $\tau_f^2\langle \omega^2|\xi\rangle$ sampled from the present DNS data appear to be controlled by the smallest turbulent structures of the Kolmogorov scale, which is much less than δ_L under conditions of the analyzed DNS.

Third, Fig. 4 also shows very weak variations of strain rate a_t within flamelets (PDFs conditioned to different ξ are barely distinguishable in Fig. 4a); a weak decrease (increase) in fluctuations of S^2 with increasing ξ if $\xi > 0.3$ ($\xi < 0.3$, respectively), as the PDFs in Fig. 4b become narrower (wider, respectively); and an increase in fluctuations of ω^2 with increasing c_F (the PDFs become wider in Fig. 4c), which is most pronounced at $\xi < 0.4$.

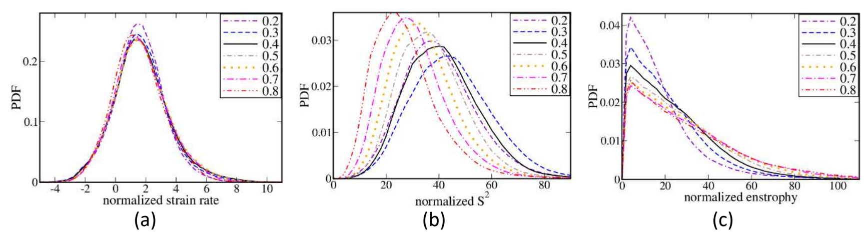

Fig. 4. Probability density functions for normalized (a) strain rate $\tau_f a_t$, (b) rate of strain $\tau_f^2 S^2$, and (c) enstrophy $\tau_f^2\omega^2$, conditioned to the local values of $c_F(\mathbf{x},t)$ specified in legends and sampled from the entire computational domain at 55 instants.

Thus, decay of small-scale turbulence within flamelets is indicated neither in Fig. 3 nor in Fig. 4. Accordingly, the constriction of PDFs of local combustion characteristics (i.e., a decrease in the magnitude of fluctuations of these characteristics) with increasing ξ, observed at $0.3 < \xi < 0.7$ in Figs. 1 and 2, should not be attributed to decay of small-scale turbulence within flamelets, as often believed. Therefore, to resolve this conundrum and to make Figs. 1 and 2 consistent with Figs. 3 and 4, another cause of reduction of the influence of small-scale turbulence on the local flamelet structure, shown in Figs. 1 and 2, should be revealed. Rapid flow acceleration, mentioned earlier by Poludnenko and Oran,[34] appears to be a relevant physical mechanism.

Indeed, if following activation energy asymptotic theories of stretched laminar flames,[48,49] we consider strain rate a_t to be the most appropriate quantity for characterizing the influence of turbulence on premixed flame structure, Fig. 3b shows that a product of $\tau_f\langle a_t|\xi\rangle$ is about (but less than) two.

However, due to rapid acceleration of the flow, caused by combustion-induced thermal expansion, the residence time $\tau_r(0.3 < c_F < 0.7)$ of turbulent structures within flamelet zones characterized by $0.3 < c_F < 0.7$ should be substantially shorter than τ_f. In the following, if the opposite is not stated, this residence time will be designated with symbol τ_r without parentheses for brevity. Therefore, a product of $\tau_r \langle a_t | c_F \rangle$ is expected to be less than unity so that the turbulence does not have time enough to significantly perturb the local flamelet structure at $0.3 < c_F < 0.7$.

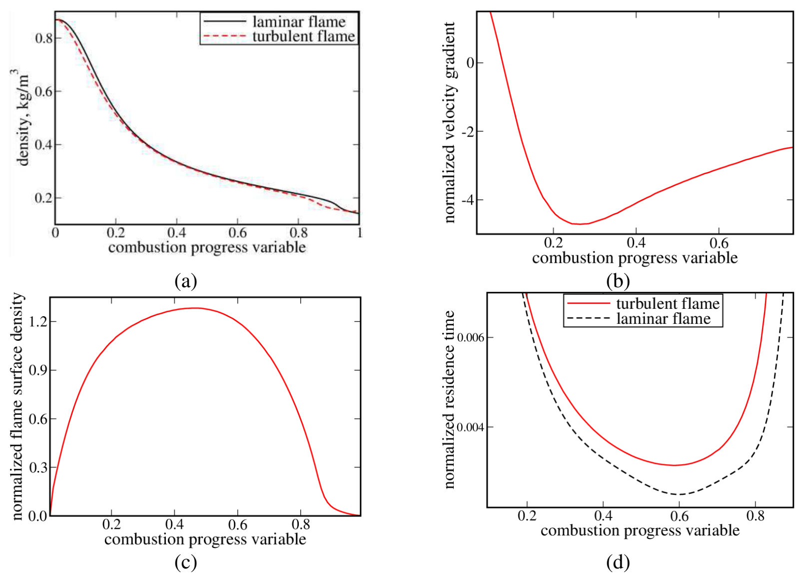

Figure 5. (a) Variations in the density in the unperturbed laminar flame (black solid line) and the conditioned density $\langle \rho | \xi \rangle$ in the turbulent flame (red dashed line). (b) Normalized conditioned derivative $\tau_f \langle \mathbf{n} \cdot \nabla(\mathbf{u} \cdot \mathbf{n}) | \xi \rangle$ of the locally normal velocity $\mathbf{u} \cdot \mathbf{n}$, taken along the local flamelet normal. (c) Normalized conditioned flame surface density $\delta_L \langle |\nabla c_F| | \xi \rangle$. (d) Normalized residence time $\tau_r(c_F)/\tau_f$ in turbulent flamelet (red solid line) and laminar flame (black dashed line) zones bounded by $c_F - 0.005$ and $c_F + 0.005$.

Density variations reported in Fig. 5a seem to indirectly support this hypothesis. Indeed, Fig. 5a shows that the local density is decreased by a factor of two already at $c_F = 0.2$ or by a factor of larger than three at $c_F = 0.6$. Consequently, the local normal flow velocity with respect to flamelets is increased (when compared to S_L) by a factor of two at $c_F = 0.2$ or by a factor of larger than three at $c_F = 0.6$. Under conditions of the present DNS, differences in density-weighted displacement speed $S_d^* = \rho S_d / \rho_u$ and S_L are statistically weak[39] and flamelets statistically retain the unperturbed laminar flame structure,[40,41] see Fig. 5a also, thus, supporting the use of the velocity $\rho_u S_L/\rho$ for estimating the residence time. It is also worth noting that the dependence of $\langle\rho|\xi\rangle$ on ξ, plotted in Fig. 5a, is significantly steeper at $\xi < 0.3$ than at larger ξ. Accordingly, by virtue of $S_d \approx \rho_u S_L/\rho$, the local increase in S_d with increasing c_F should be more pronounced (statistically) at $c_F < 0.3$. Therefore, the rate of reduction of the influence of turbulence on the local flamelet structure should be higher (statistically) at low c_F. Indeed, such a trend is observed for the rate $\dot{\omega}_T(\mathbf{x},t)$ in Fig. 1c and, especially, for $Y_H(\mathbf{x},t)$ in Fig. 1b.

Significant acceleration of the locally normal flow in flamelet zones characterized by $0.2 < c_F < 0.7$ is further supported in Fig. 5b, which shows the normalized conditioned derivative $\tau_f\langle\mathbf{n}\cdot\nabla(\mathbf{u}\cdot\mathbf{n})|\xi\rangle$ of the locally normal velocity $\mathbf{u}\cdot\mathbf{n}$, taken along the local flamelet normal $\mathbf{n}$. Here, the negative derivative indicates acceleration of the flow in the direction opposite to $\mathbf{n}$, i.e., to products. Due to the rapid acceleration of the locally normal flow, the residence time of turbulent fluid within the discussed flamelet zone ($0.2 < c_F < 0.7$) should be reduced. In addition, the residence is relatively short due to a small thickness of this zone due to large local values of $|\nabla c_F|$, see Fig. 5c.

The joint effect of these two factors (large local $|\langle\mathbf{n}\cdot\nabla(\mathbf{u}\cdot\mathbf{n})|\xi\rangle|$ and large local $|\nabla c_F|$) is illustrated in Fig. 5d, which reports variations of the normalized residence time $\tau_r(c_F)/\tau_f$ in the laminar flame zones bounded by $c_F \pm \Delta c_F$ where $\Delta c_F = 0.005$, see black solid line. This normalized time, evaluated as follows

$$\frac{\tau_r(c_F)}{\tau_f} = \frac{1}{\tau_f u(x)}\frac{\Delta c_F}{|dc_F/dx|}, \tag{2}$$

is much less than unity, partially because it characterizes thin zones associated with $\Delta c_F = 0.01$. However, even the residence time τ_r in a significantly thicker zone of $0.195 < c_F < 0.705$, which has been estimated to be a sum of residence times evaluated using Eq. (2) for $c_F = 0.2 \pm \Delta c_F$, $c_F = 0.21 \pm \Delta c_F$, …, and $c_F = 0.7 \pm \Delta c_F$, is equal to $0.18\tau_f$, whereas the Kolmogorov time scale τ_K evaluated at the leading edge of the mean flame brush is larger by a factor of 2.5. This comparison of τ_r and τ_K supports a hypothesis that the residence time is too short and even the smallest-scale turbulent fluctuations creating the largest velocity gradients do not have enough time to significantly perturb the local flamelet structure at $0.2 < c_F < 0.7$. When c_F tends to zero or unity, the local residence time rapidly grows. For instance, it is equal to $0.42\tau_f$ and $1.07\tau_f$ for $0.02 < c_F < 0.2$ and $0.7 < c_F < 0.98$, respectively. Accordingly, the influence of small-scale turbulence on local flamelet structure is more pronounced at low and large c_F.

While black dashed line in Fig. 5d shows results obtained from the laminar flame, these results characterize the residence time within turbulent flamelets to the leading order, because the flamelet structure is weakly perturbed from the statistical perspective under conditions of the present DNS study, as shown earlier,[40,41] see Fig. 5a also. In addition, the following simplified estimate

$$\frac{\tau_r(\xi)}{\tau_f} = \frac{1}{\tau_f u(n)} \frac{\Delta\xi}{\langle|\nabla c_F||\xi\rangle}, \qquad u(n) = S_L - \int_{c_F^*}^{\xi} \langle \mathbf{n}\cdot\nabla(\mathbf{u}\cdot\mathbf{n})|\zeta\rangle \frac{d\zeta}{\langle|\nabla c_F||\zeta\rangle}, \tag{3}$$

of the normalized residence time within turbulent flamelets was also performed. Here, when compared to Eq. (2), (i) distance along the locally normal (to the flamelet) direction is estimated to be equal to $\Delta\xi/\langle|\nabla c_F||\xi\rangle$, (ii) flow velocity in the laminar flow is substituted with the locally normal flow velocity $u(n)$, (iii) which is estimated by integrating the locally normal velocity gradient $\langle \mathbf{n}\cdot\nabla(\mathbf{u}\cdot\mathbf{n})|\zeta\rangle$ along the normal direction, with (iv) the integration being performed starting from a value of ξ, associated with the change of the sign of $\langle \mathbf{n}\cdot\nabla(\mathbf{u}\cdot\mathbf{n})|\xi\rangle$ from positive at $\xi < c_F^*$ (in such flamelet zones, turbulent fluctuations of velocity statistically overwhelm velocity changes due to the local density variations) to negative at $\xi > c_F^*$ (in such flamelet zones, local acceleration of the normal flow is mainly controlled by heat release). Due to the significant influence of turbulent velocity fluctuations on $\langle \mathbf{n}\cdot\nabla(\mathbf{u}\cdot\mathbf{n})|\xi\rangle$ at low ξ, the choice of the integration boundary c_F^* is not rigorous. Accordingly, a correlation between velocity and scalar gradients is also neglected in Eq. (2), i.e., the conditioned ratio $\langle \mathbf{n}\cdot\nabla(\mathbf{u}\cdot\mathbf{n})/|\nabla c_F|\,|\xi\rangle$ is substituted with the ratio $\langle \mathbf{n}\cdot\nabla(\mathbf{u}\cdot\mathbf{n})|\xi\rangle/\langle|\nabla c_F||\xi\rangle$ of conditioned quantities. Nevertheless, the residence times calculated using Eqs. (1) and (2) are close to one another at $0.2 < \xi < 0.7$, thus, further supporting the residence-time hypothesis.

This hypothesis could also be useful for understanding the lack of substantial decay of various turbulence characteristics as turbulent structures move from $c_F = 0.2$ to $c_F = 0.7$ within flamelets, see Figs. 3 and 4. For instance, the residence time could be insufficient for the dissipation of turbulence due to molecular viscosity to substantially decrease magnitudes of local velocity gradients. If we (i) estimate time required for this dissipation as follows $\tau_\varepsilon = (\nu/\varepsilon)^{1/2}$, (ii) take the highest value of the conditioned dissipation rate $\nu_u^{-1}\tau_f^2\langle\varepsilon|\xi\rangle = 93$, reported in Fig. 3c, and (iii) allow for an increase in the viscosity ν at $\xi = 0.6$ or $T = 1130$ K, associated with this highest value, i.e., $\nu(c_F = 0.6) = 2.5\nu_u$; we obtain the dissipation time scale that is shorter by a factor of 2.7 than the Kolmogorov time scale τ_K evaluated at the leading edge of the mean flame brush. Therefore, the dissipation time scale can be as low as $0.9\tau_r$ and magnitude of velocity gradients could be decreased by viscous dissipation, e.g., see red solid line in Fig. 3c (at $\xi > 0.3$) or PDFs reported in Fig. 4b. However, since even the shortest dissipation time scale is comparable with the residence time τ_r, the observed decrease in $\tau_f^2\langle S^2|\xi\rangle$ with ξ is sufficiently slow. Moreover, the influence of combustion-induced thermal expansion on a turbulent flow is not reduced to an increase in the kinematic viscosity with the temperature and other physical mechanisms discussed in detail elsewhere[50,51] can also play an important role. For instance, generation of vorticity by baroclinic torque, appears to control an increase in (i) the conditioned enstrophy $\tau_f^2\langle\omega^2|\xi\rangle$ at $0.2 < \xi < 0.8$, see black dotted-dashed line in Fig. 3c, or (ii) magnitude of its fluctuations, see Fig. 4c. Besides, generation of potential velocity gradients and reduction of vorticity due to dilatation appear to control an increase $\tau_f^2\langle S^2|\xi\rangle$ at $0.05 < \xi < 0.3$ and a decrease in $\tau_f^2\langle\omega^2|\xi\rangle$ at $\xi < 0.15$, respectively, see Fig. 3c. An analysis of these physical mechanisms will be a subject for future work but is beyond the scope of the present study. Nevertheless, the limited residence time of small-scale turbulence within flamelets could also play a role and should also be borne in mind.

IV. CONCLUDING REMARKS

DNS data analyzed in the present work show that (i) the influence of small-scale (when compared to the laminar flame thickness) turbulence on internal flamelet structure is reduced during advection from unburned reactants to combustion products, but (ii) neither the local turbulence characteristics (conditioned rms velocities, total strain, and enstrophy) nor flame strain rate decrease substantially from the reactant side to the product side. To reconcile these two apparently inconsistent trends, the former is hypothesized to stem from shortening of the residence time of the small-scale turbulence within flamelets due to combustion-induced acceleration of the local flow in the flamelet-normal direction. Certain DNS data discussed above indirectly support this hypothesis.

It is worth recalling that an apparently similar hypothesis highlighting insufficient residence time of turbulence in a flame brush was earlier put forward[52] to explain weak influence of turbulence on the surface of an unburned-mixture-finger.[53] However, the residence time considered in the cited studies is controlled by turbulent motion in unburned reactants from the leading edge of a thick mean flame brush to its trailing edge, whereas the residence time emphasized in the present work is controlled by advection of turbulence through thin flamelets.

Finally, it should be stressed that the present study does not indicate that the hypothesized residence-time mechanism always dominates, whereas a widely accepted turbulence-decay mechanism is of minor importance. Both physical mechanisms are expected to play an important role, but, likely, at different conditions. This issue requires further study, e.g., to find a criterion that separates domains of primarily importance of each mechanism. Since $S_L\delta_L/\nu_u$ and, hence, difference between $Ka = \tau_f/\tau_K$ and $(\delta_L/\eta_K)^2$ is much larger in lean or near-stoichiometric hydrogen-air flames than in hydrocarbon-air ones, conditions of the present study, i.e., $Ka = O(1)$ despite $(\delta_L/\eta_K)^2 \gg 1$, are specific to the former flames and are beneficial for the residence-time mechanism. In hydrocarbon-air flames characterized by $(\delta_L/\eta_K)^2 \gg 1$, the Karlovitz number Ka should also be much larger than unity and a decrease in the residence time of small-scale turbulence within flamelets is unlikely to make the residence time shorter than τ_K. Nevertheless, the hypothesized residence-time mechanism should be borne in mind, at least for hydrogen-air turbulent premixed flames.

Declaration of Competing Interest

The authors declare that they have no known competing financial interests or personal relationships that could have appeared to influence the work reported in this paper.

Data availability

The data that support the findings of this study are available from the corresponding author upon reasonable request.

Acknowledgements

ANL gratefully acknowledges the financial support provided by Chalmers Area of Advance Transport. VAS gratefully acknowledges the financial support provided by ONERA and the Ministry of Science and Higher Education of the Russian Federation (Grant agreement of December 8, 2020, No. 075-11-2020-023) within the program for the creation and development of the World-Class Research Center "Supersonic" for 2020-2025.

References

[1]G. Damköhler, Der einfuss der turbulenz auf die flammengeschwindigkeit in gasgemischen, *Zs. Electrochemie* 46 (1940) 601-652.

[2]K.I. Shelkin, On combustion in a turbulent flow, *Jour. Tech. Phys. USSR* 13(9-10) (1943) 520-530.

[3]A. Y. Klimenko, "The convergence of combustion models and compliance with the Kolmogorov scaling of turbulence," Phys. Fluids **33**, 025112 (2021).

[4]J. F. MacArt and M. E. Mueller, "Damköhler number scaling of active cascade effects in turbulent premixed combustion," Phys. Fluids **33**, 035103 (2021).

[5]T. Readshaw, T. Ding, S. Rigopoulos, and W. P. Jones, "Modeling of turbulent flames with the large eddy simulation–probability density function (LES–PDF) approach, stochastic fields, and artificial neural networks," Phys. Fluids **33**, 035154 (2021).

[6]V. A. Sabelnikov and A. N. Lipatnikov, "Scaling of reaction progress variable variance in highly turbulent reaction waves," Phys. Fluids **33**, 085103 (2021).

[7]N. Chakraborty, C. Kasten, U. Ahmed, and M. Klein, "Evolutions of strain rate and dissipation rate of kinetic energy in turbulent premixed flames," Phys. Fluids **33**, 125132 (2021).

[8]H. C. Lee, P. Dai, M. Wan, and A. N. Lipatnikov, "Lewis number and preferential diffusion effects in lean hydrogen–air highly turbulent flames," Phys. Fluids **34**, 035131 (2022).

[9]A. N. Lipatnikov and V. A. Sabelnikov, "Flame folding and conditioned concentration profiles in moderately intense turbulence," Phys. Fluids **34**, 065119 (2022).

[10]N. Chakraborty, U. Ahmed, M. Klein, and H. G. Im, "Alignment statistics of pressure Hessian with strain rate tensor and reactive scalar gradient in turbulent premixed flames," Phys. Fluids **34**, 065120 (2022).

[11]V. A. Sabelnikov, A. N. Lipatnikov, N. Nikitin, F. E. Hernández-Pérez, and H. G. Im, "Conditioned structure functions in turbulent hydrogen/air flames," Phys. Fluids **34**, 085103 (2022).

[12]V. A. Sabelnikov, A. N. Lipatnikov, N. Nikitin, F. E. Hernández-Pérez, and H. G. Im, "Effects of thermal expansion on moderately intense turbulence in premixed flames," Phys. Fluids **34**, 115127 (2022).

[13]R. Borghi, "On the structure and morphology of turbulent premixed flames," in *Recent Advances in Aerospace Science*, edited by S. Casci and C. Bruno (New York: Plenum, 1984), pp. 117-138.

[14]F.A. Williams, *Combustion Theory*, 2nd ed. (Benjamin/Cummings, Menlo Park, California, 1985).

[15]N. Peters, "Laminar flamelet concepts in turbulent combustion," Proc. Combust. Inst. **21**, 1231 (1986).

[16]A. S. Monin and A. M. Yaglom, *Statistical Fluid Mechanics: Mechanics of Turbulence*, vol. 2 (The MIT Press, Cambridge, Massachusetts, 1975).

[17]L. D. Landau and E. M. Lifshitz, *Fluid Mechanics* (Pergamon Press, Oxford, UK, 1987).

[18]N. Peters, *Turbulent Combustion* (Cambridge Univ. Press, Cambridge, UK, 2000).

[19]T. Poinsot and D. Veynante, *Theoretical and Numerical Combustion*, 2nd ed. (Edwards, Philadelphia, 2005).

[20]A. N. Lipatnikov, *Fundamentals of Premixed Turbulent Combustion* (CRC Press, Boca Raton, Florida, 2012).

[21]N. Peters, "The turbulent burning velocity for large-scale and small-scale turbulence," J. Fluid Mech. **384**, 107 (1999).

[22]Ya. B. Zel'dovich, G. I. Barenblatt, V. B. Librovich, and G. M. Makhviladze, *The Mathematical Theory of Combustion and Explosions* (Consultants Bureau, New York, 1985).

[23]A. N. Lipatnikov and V. A. Sabelnikov, "Karlovitz numbers and premixed turbulent combustion regimes for complex-chemistry flames," *Energies* **15**, 5840 (2022).

[24]J. F. Driscoll, "Turbulent premixed combustion: flamelet structure and its effect on turbulent burning velocities," Prog. Energy Combust. Sci. **34**, 91 (2008).

[25]V. A. Sabelnikov, R. Yu, and A. N. Lipatnikov, "Thin reaction zones in constant-density turbulent flows at low Damköhler numbers: Theory and simulations," Phys. Fluids **31**, 055104 (2019).

[26]J. F. Driscoll, J. H. Chen, A. W. Skiba, C. D. Carter, E. R. Hawkes, and H. Wang, "Premixed flames subjected to extreme turbulence: Some questions and recent answers," Prog. Energy Combust. Sci. **76**, 100802 (2020).

[27]Q. Fan, X. Liu, L. Xu, A. A. Subash, C. Brackmann, M. Aldén, X.-S. Bai, and Z. Li, "Flame structure and burning velocity of ammonia/air turbulent premixed flames at high Karovitz number conditions," Combust. Flame **238**, 111943 (2022).

[28]Q. Fan, X. Liu, X. Cai, C. Brackmann, M. Aldén, X.-S. Bai, and Z. Li, "Structure and scalar correlation of ammonia/air turbulent premixed flames in the distributed reaction zone regime," Combust. Flame **241**, 112090 (2022).

[29]A. W. Skiba, T. M. Wabel, C. D. Carter, S. D. Hammack, J. E. Temme, and J. F. Driscoll, "Premixed flames subjected to extreme levels of turbulence part I: Flame structure and a new measured regime diagram," Combust. Flame **189**, 407 (2018).

[30]T. Poinsot, D. Veynante, and S. Candel, "Quenching processes and premixed turbulent combustion diagrams," J. Fluid Mech. **228**, 561 (1991).

[31]P.-H. Renard, D. Thévenin, J. C. Rolon, and S. Candel, "Dynamics of flame/vortex interactions," Prog. Energy Combust. Sci. **26**, 225 (2000).

[32]P. L. K. Paes, Y. G. Shah, J. G. Brasseura, and Y. Xuan, "A scaling analysis for the evolution of small-scale turbulence eddies across premixed flames with implications on distributed combustion," Combust. Theory Modell. **24**, 307 (2020).

[33]S. Luna and F. N. Egolfopoulos, "Local effects in vortex-flame interactions: Implications for turbulent premixed flame scaling and observables," Combust. Flame **245**, 112293 (2022).

[34]A. Y. Poludnenko and E. S. Oran, "The interaction of high-speed turbulence with flames: Global properties and internal flame structure," Combust. Flame **157**, 995 (2010).

[35]A.J. Aspden, "A numerical study of diffusive effects in turbulent lean premixed hydrogen flames," Proc. Combust. Inst. **36**, 1997 (2017).

[36]N. A. K. Doan, N. Swaminathan, and "Multiscale analysis of turbulence-flame interaction in premixed flames," Proc. Combust. Inst. **36**, 1929 (2017).

[37]T. M. Wabel, A. W. Skiba, and J. F. Driscoll, "Evolution of turbulence through a broadened preheat zone in a premixed piloted Bunsen flame from conditionally-averaged velocity measurements," Combust. Flame 188, 13 (2018).

[38]H. L. Dave, A. Mohan, and S. Chaudhuri, "Genesis and evolution of premixed flames in turbulence," Combust. Flame **196**, 386 (2018).

[39]H. L. Dave and S. Chaudhuri, "Evolution of local flame displacement speeds in turbulence," J. Fluid Mech. **884**, A46 (2020).

[40]A. N. Lipatnikov and V. A. Sabelnikov, "An extended flamelet-based presumed probability density function for predicting mean concentrations of various species in premixed turbulent flames," Int. J. Hydrogen Energy **45**, 31162 (2020).

[41]A. N. Lipatnikov and V. A. Sabelnikov, "Evaluation of mean species mass fractions in premixed turbulent flames: A DNS study," Proc. Combust. Inst. **38**, 6413 (2021).

[42]V. A. Sabelnikov, A. N. Lipatnikov, S. Nishiki, H. L. Dave, F. E. Hernández-Pérez, W. Song, and H. G. Im, "Dissipation and dilatation rates in premixed turbulent flames," Phys. Fluids **33**, 035112 (2021).

[43]A. N. Lipatnikov and V. A. Sabelnikov, "Flame folding and conditioned concentration profiles in moderately intense turbulence," Phys. Fluids **34**, 065119 (2022).

[44]J. Li, Z. Zhao, A. Kazakov, and F. L. Dryer, "An updated comprehensive kinetic model of hydrogen combustion," Int. J. Chem. Kinetics **36**, 566 (2004).

[45]N. Babkovskaia, N. E. L. Haugen, and A. Brandenburg, "A high-order public domain code for direct numerical simulations of turbulent combustion," J. Comput. Phys. **230**, 1 (2011).

[46]T. J. Poinsot and S. K. Lele, "Boundary conditions for direct simulations of compressible viscous flows," J. Comput. Phys. **101**, 104 (1992).

[47]F. A. Williams, "Progress in knowledge of flamelet structure and extinction," Prog. Energy Combust. Sci. **26**, 657 (2000).

[48]M. Matalon, "On flame stretch," Combust. Sci. and Technol. **31**, 169 (1983).

[49]P. Clavin, "Dynamical behavior of premixed flame fronts in laminar and turbulent flows," Prog. Energy Combust. Sci. **11**, 1 (1985).

[50]A. N. Lipatnikov and J. Chomiak, "Effects of premixed flames on turbulence and turbulent scalar transport," Prog. Energy Combust. Sci. **36**, 1 (2010).

[51]V. A. Sabelnikov and A. N. Lipatnikov, "Recent advances in understanding of thermal expansion effects in premixed turbulent flames," Annu. Rev. Fluid Mech. **49**, 91 (2017).

[52]A. N. Lipatnikov, J. Chomiak, V. A. Sabelnikov, S. Nishiki, and T. Hasegawa, "A DNS study of the physical mechanisms associated with density ratio influence on turbulent burning velocity in premixed flames," Combust. Theory Modell. **22**, 131 (2018).

[53]A. N. Lipatnikov, J. Chomiak, V. A. Sabelnikov, S. Nishiki, and T. Hasegawa, "Unburned mixture fingers in premixed turbulent flames," Proc. Combust. Inst. **35**, 1401 (2015).

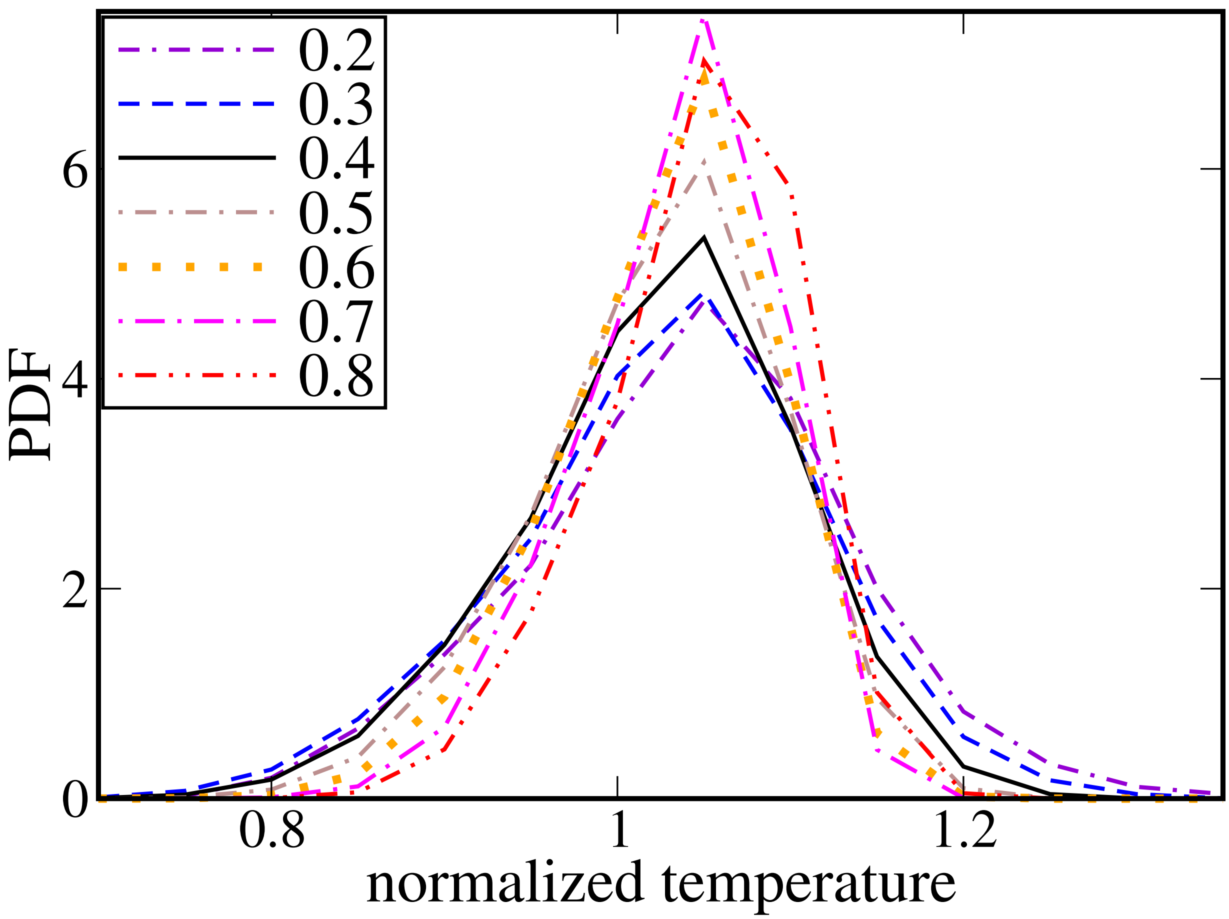
0.2
0.3
0.4
0.5
0.6
0.7
0.8
PDF
0
2
4
6
0.8
1
1.2
normalized temperature

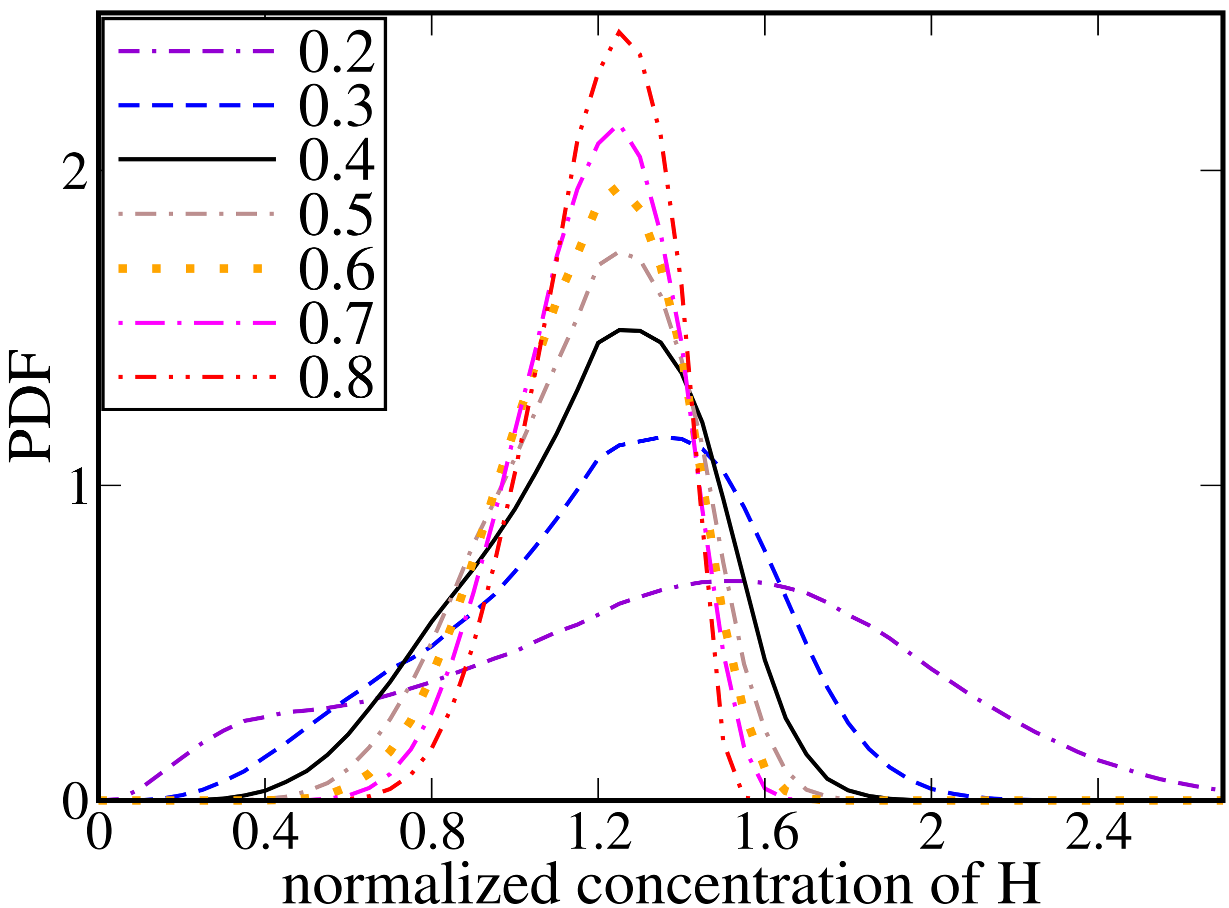
0.2
0.3
0.4
0.5
0.6
0.7
0.8
PDF
0
1
2
0
0.4
0.8
1.2
1.6
2
2.4
normalized concentration of H

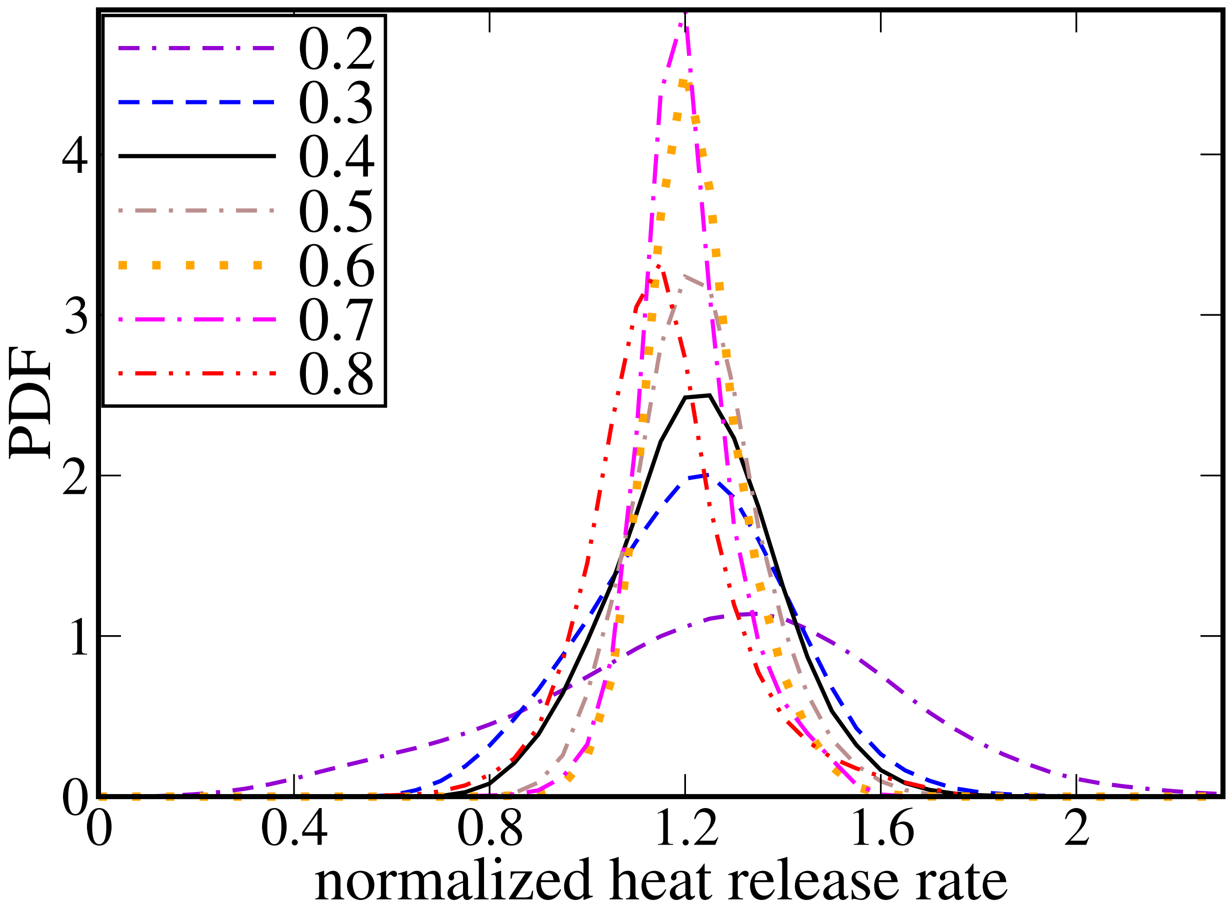
0.2
0.3
0.4
0.5
0.6
0.7
0.8
PDF
0
1
2
3
4
0
0.4
0.8
1.2
1.6
2
normalized heat release rate

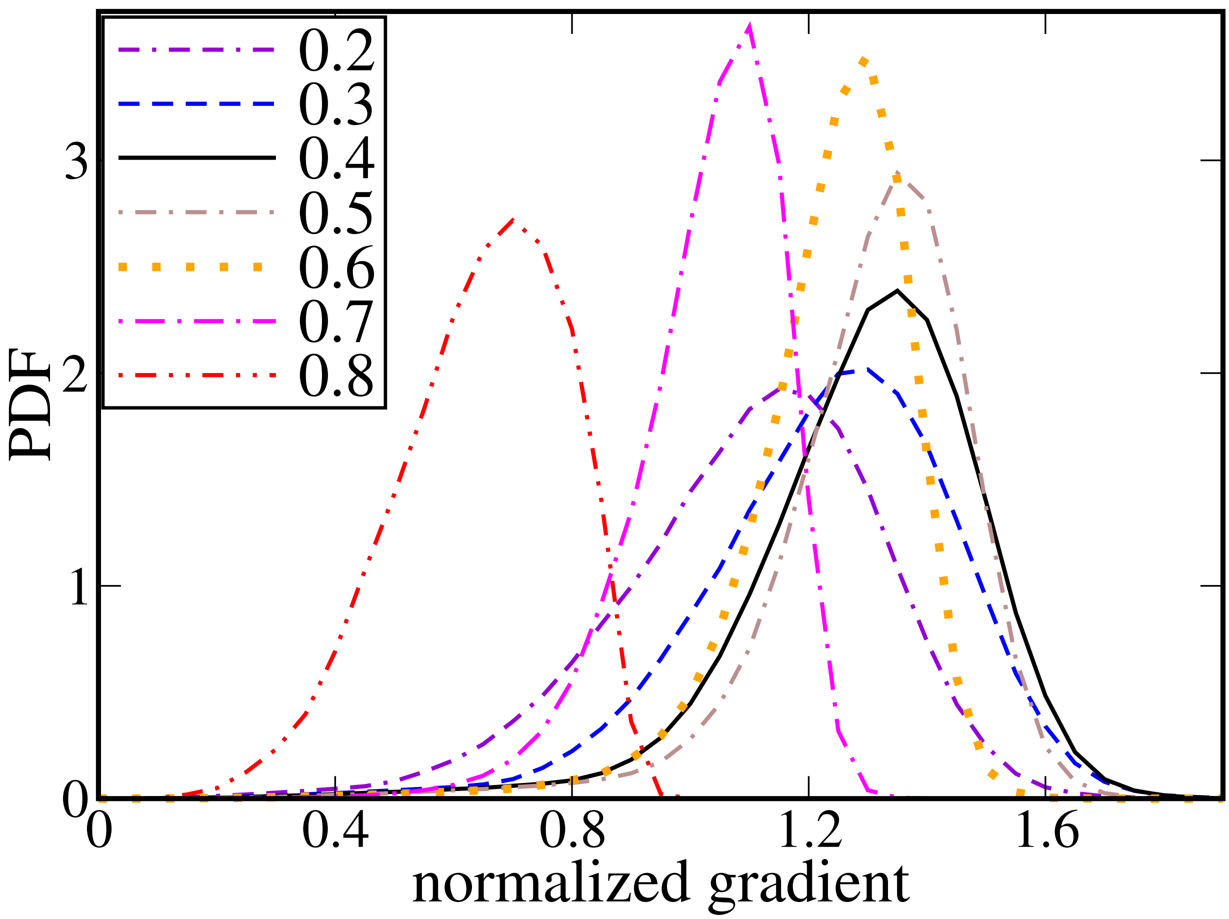
0.2
0.3
0.4
0.5
0.6
0.7
0.8
PDF
normalized gradient
0
1
2
3
0
0.4
0.8
1.2
1.6

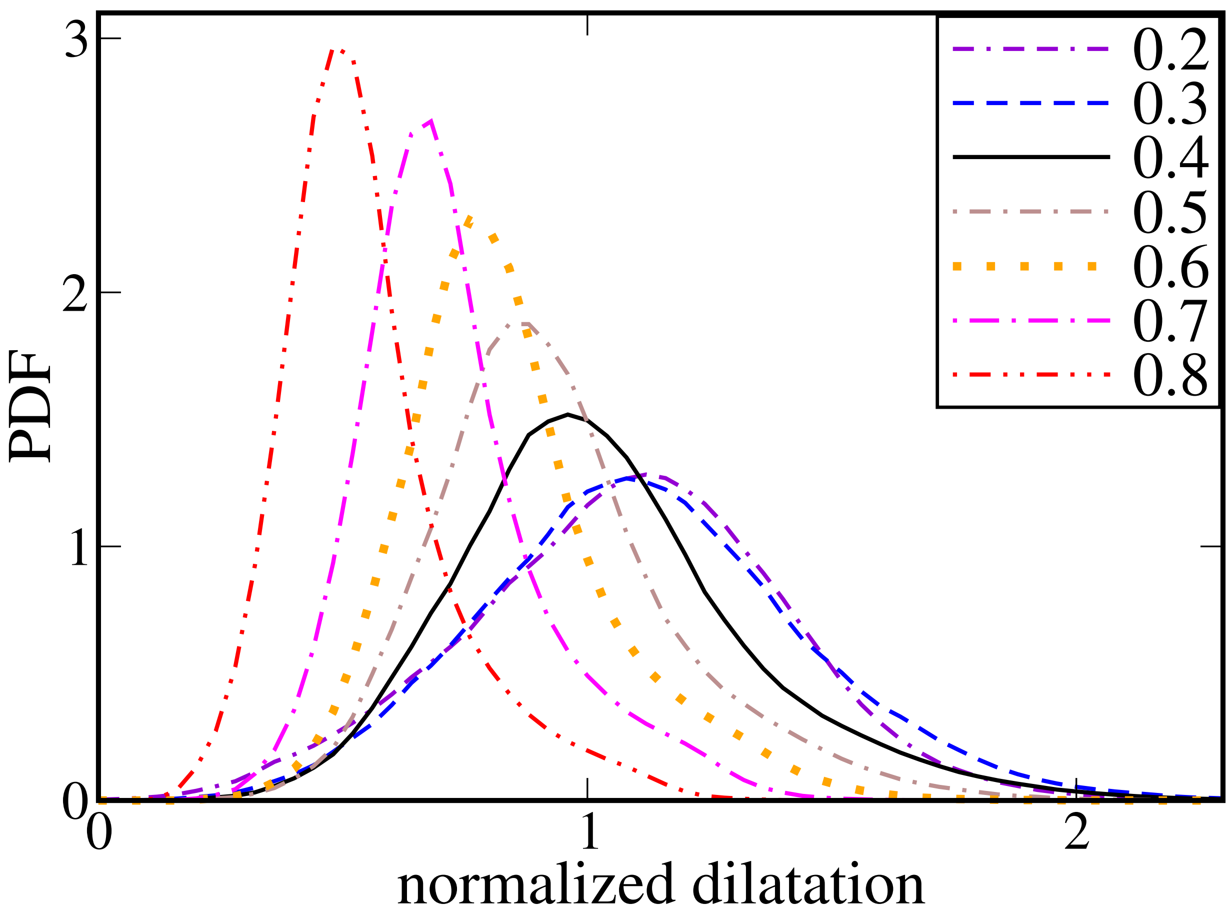
PDF
normalized dilatation
0
1
2
3
0
1
2
0.2
0.3
0.4
0.5
0.6
0.7
0.8

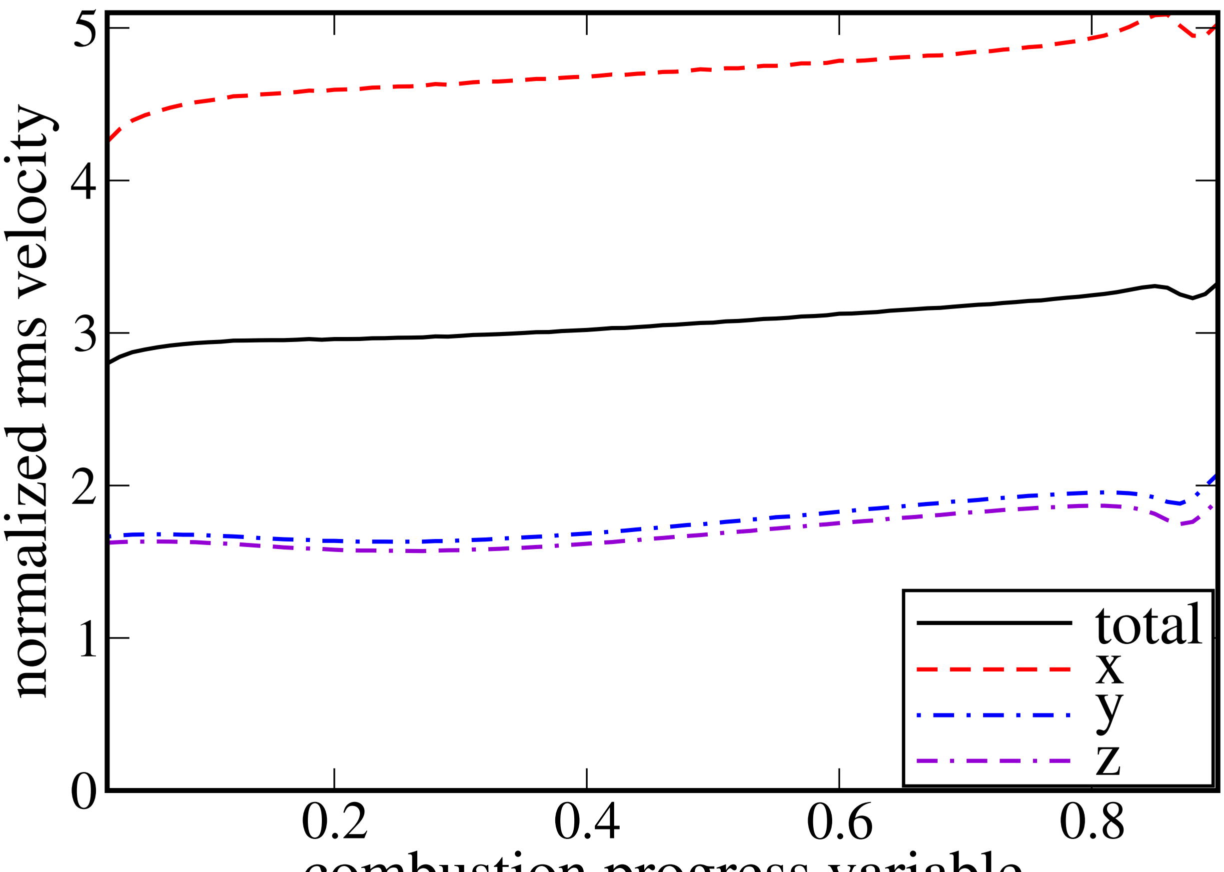
normalized rms velocity
combustion progress variable
0
1
2
3
4
5
0.2
0.4
0.6
0.8
total
x
y
z

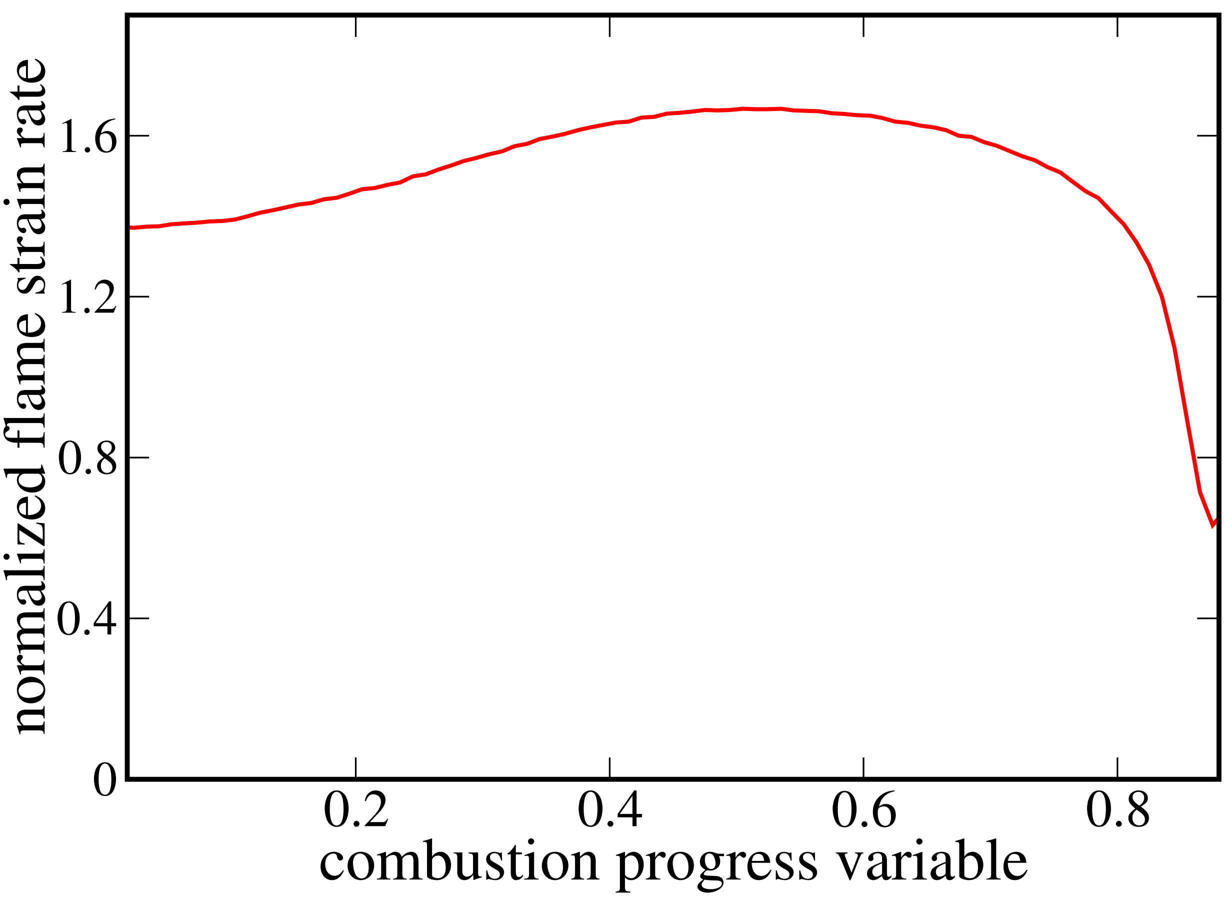
normalized flame strain rate
combustion progress variable
0
0.4
0.8
1.2
1.6
0.2
0.4
0.6
0.8

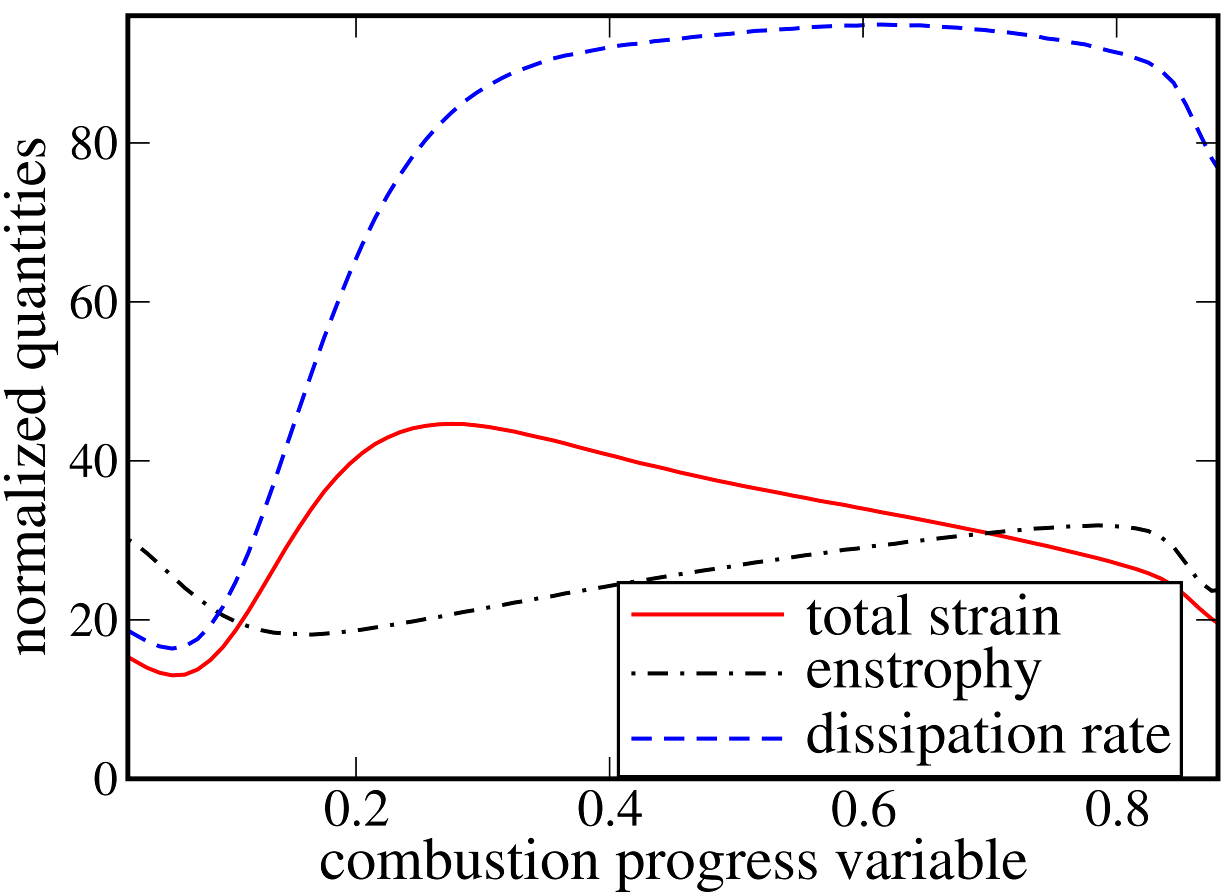
normalized quantities
0
20
40
60
80
0.2
0.4
0.6
0.8
combustion progress variable
total strain
enstrophy
dissipation rate

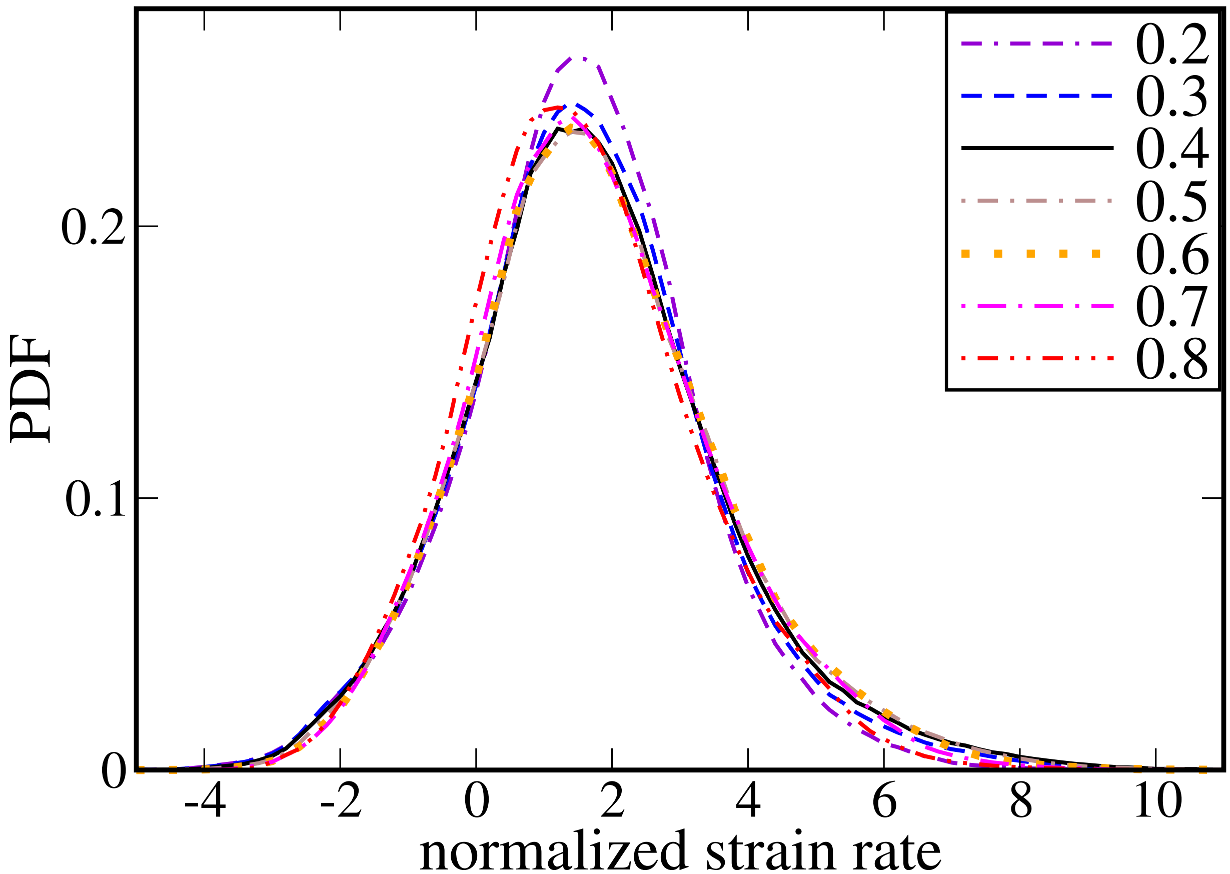
0.2
0.3
0.4
0.5
0.6
0.7
0.8
PDF
0
0.1
0.2
-4
-2
0
2
4
6
8
10
normalized strain rate

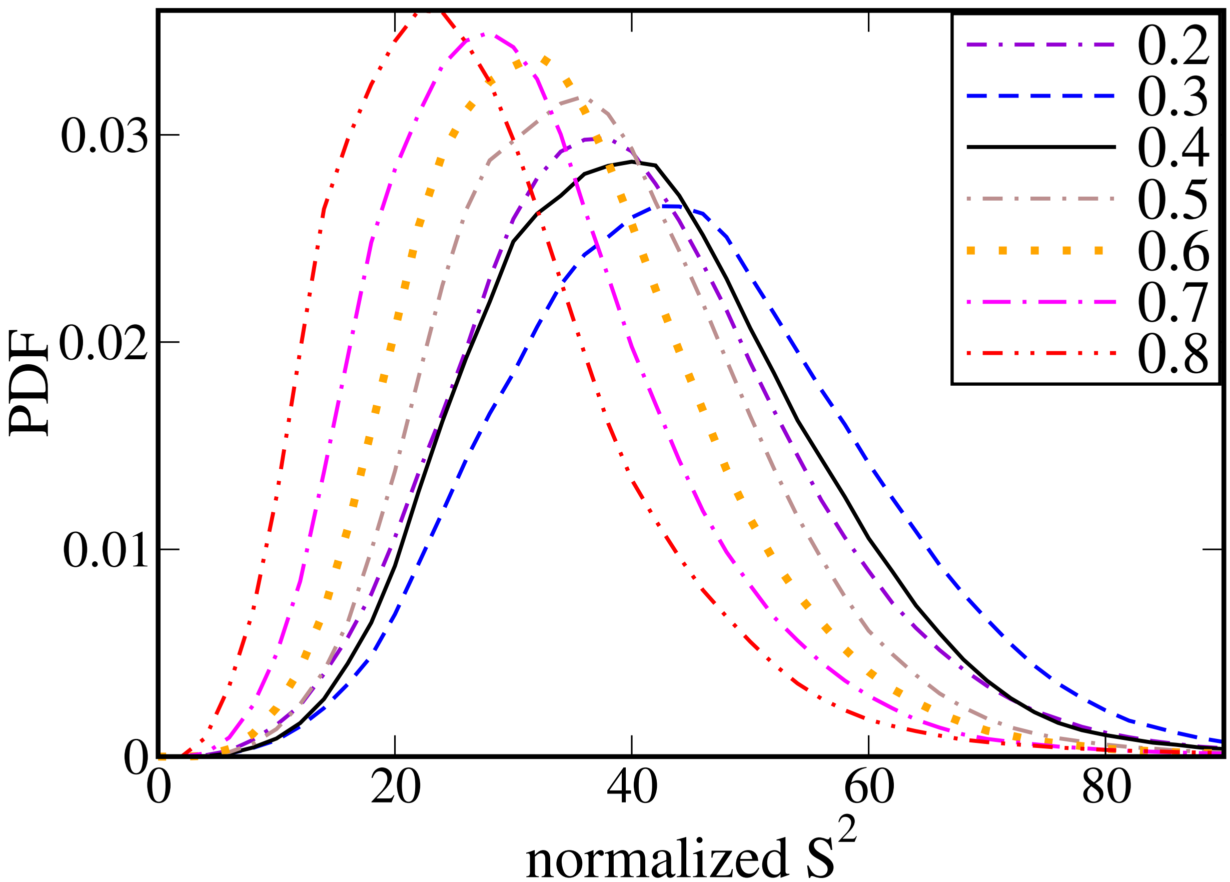
0.2
0.3
0.4
0.5
0.6
0.7
0.8
PDF
0.03
0.02
0.01
0
0
20
40
60
80
normalized S^2

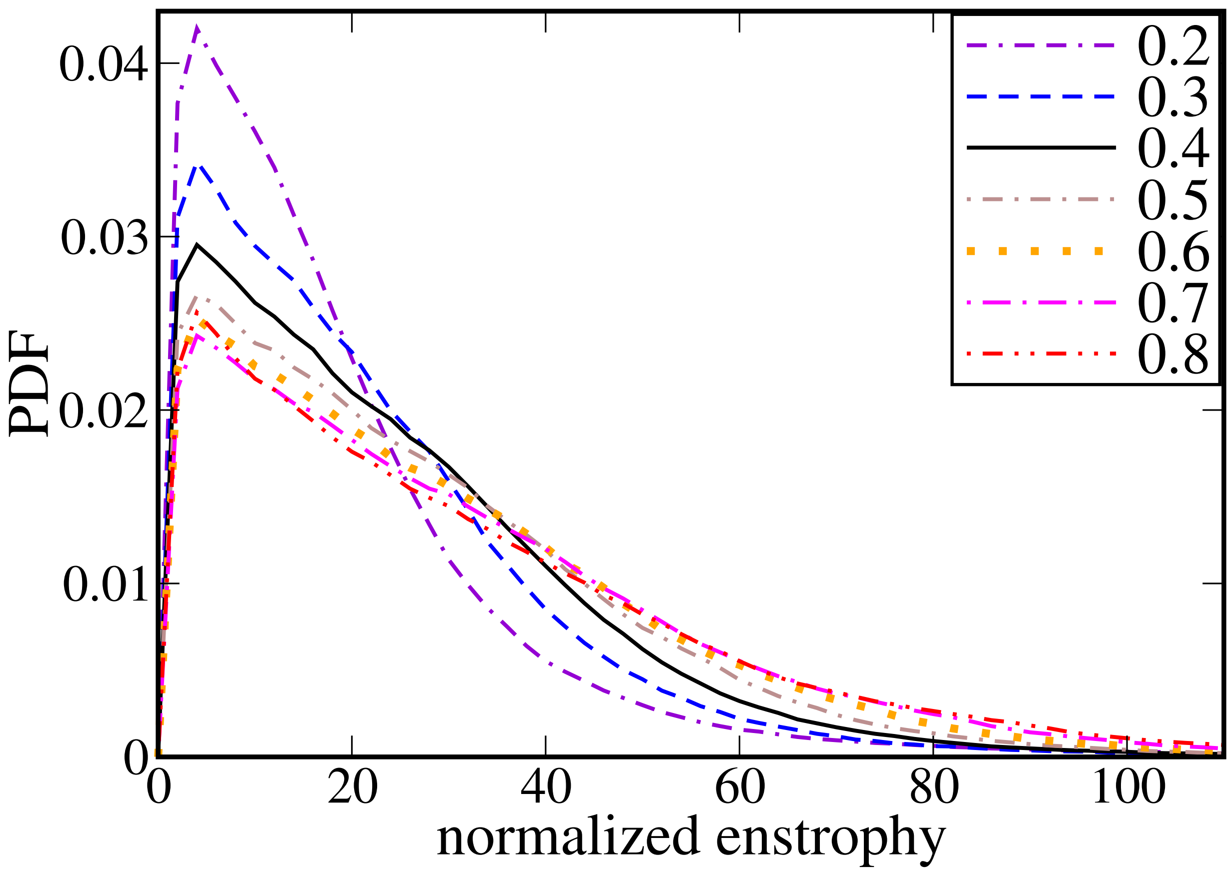
PDF
normalized enstrophy
0
0.01
0.02
0.03
0.04
0
20
40
60
80
100
0.2
0.3
0.4
0.5
0.6
0.7
0.8

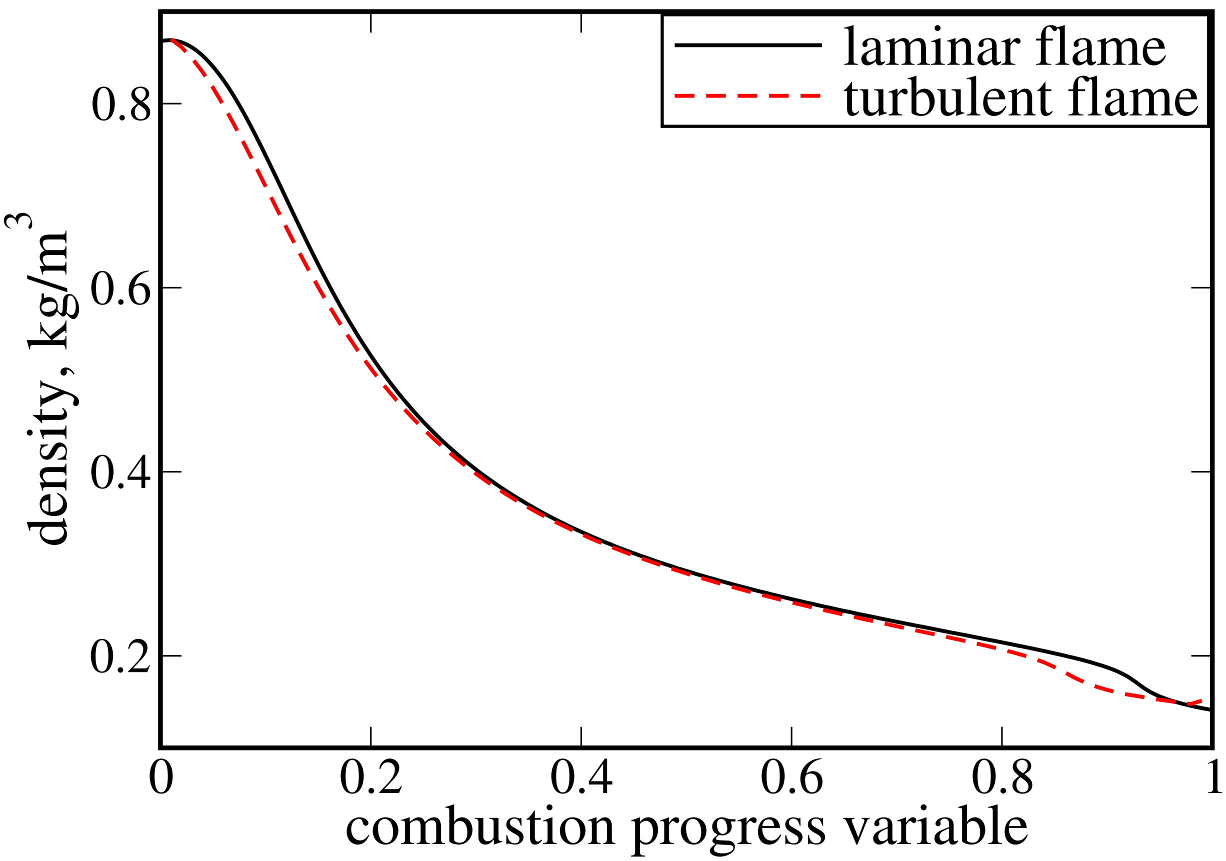
laminar flame
turbulent flame
density, kg/m^3
0.8
0.6
0.4
0.2
0
0.2
0.4
0.6
0.8
1
combustion progress variable

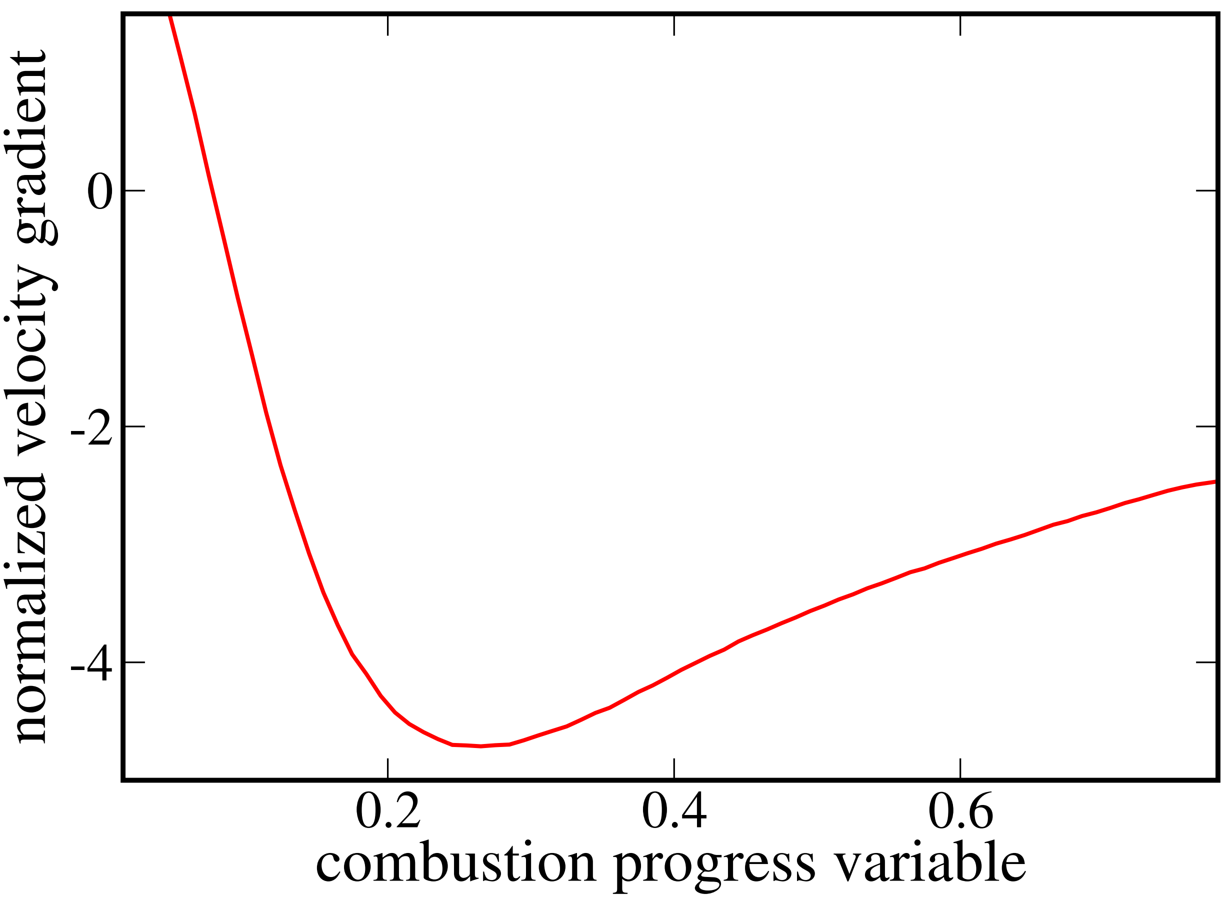
normalized velocity gradient
0
-2
-4
0.2
0.4
0.6
combustion progress variable

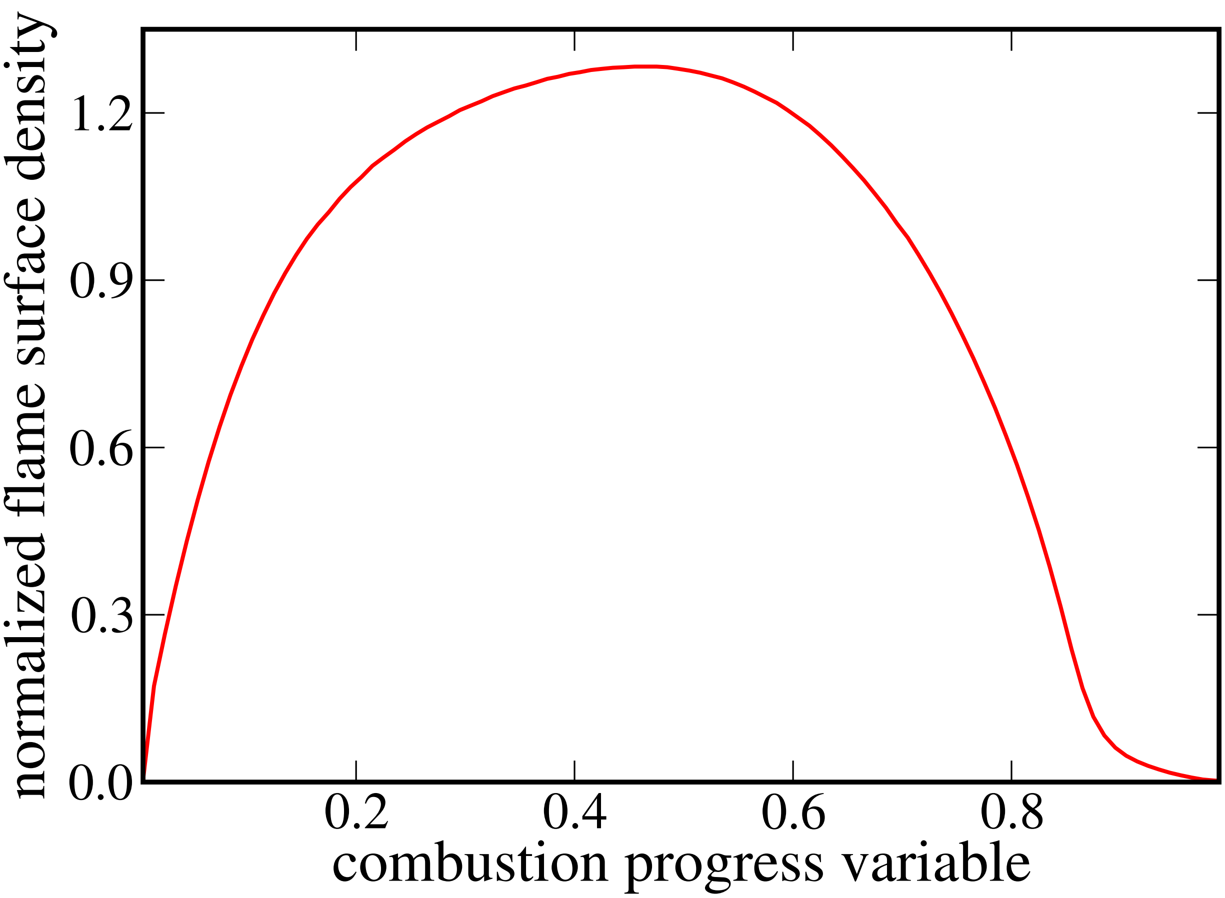
normalized flame surface density
1.2
0.9
0.6
0.3
0.0
0.2
0.4
0.6
0.8
combustion progress variable

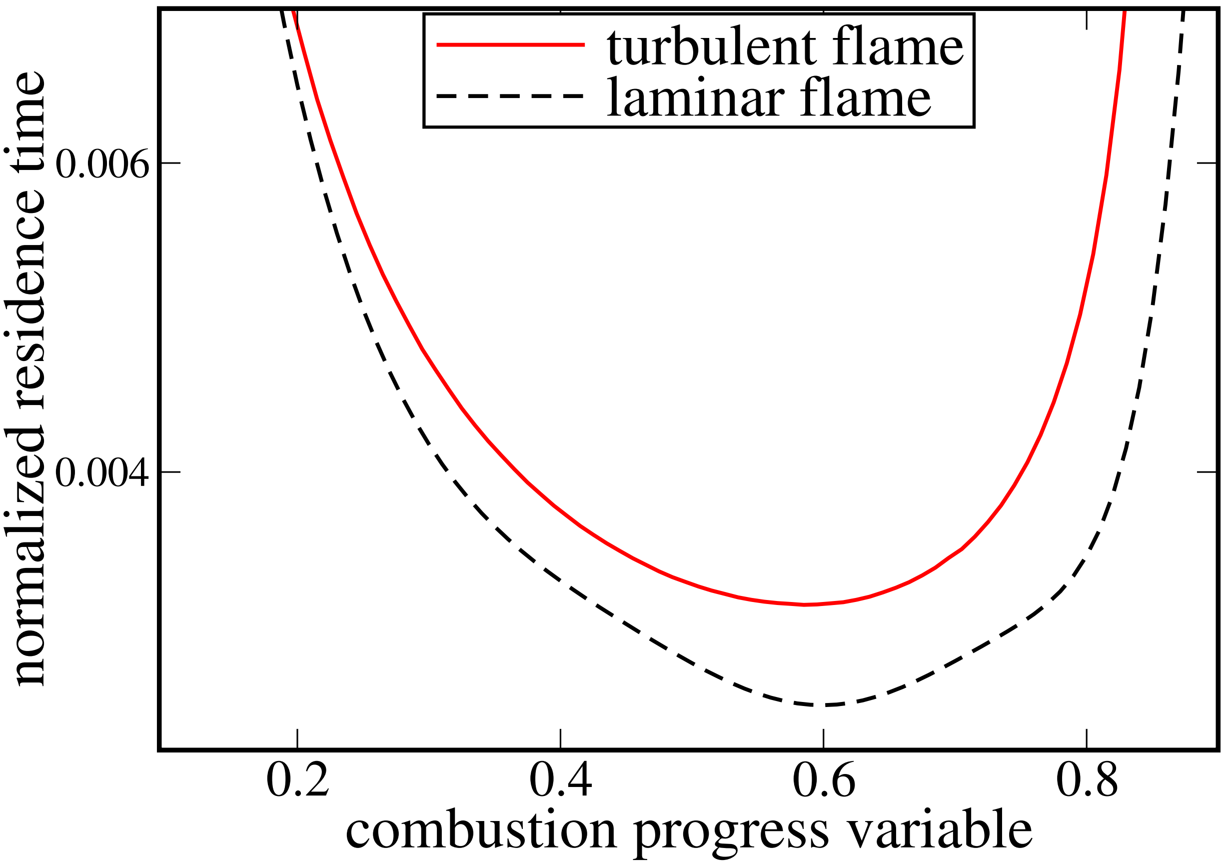
turbulent flame
laminar flame
normalized residence time
0.006
0.004
0.2
0.4
0.6
0.8
combustion progress variable